MEAN-FIELD RENORMALIZATION GROUP THEORY OF THE *t-J* MODEL

A THESIS

SUBMITTED TO THE DEPARTMENT OF PHYSICS

AND THE INSTITUTE OF ENGINEERING AND SCIENCE

OF BILKENT UNIVERSITY

IN PARTIAL FULFILLMENT OF THE REQUIREMENTS

FOR THE DEGREE OF

MASTER OF SCIENCE

By

Cengiz Şen

July, 2002

I certify that I have read this thesis and that in my opinion it is fully adequate, in scope and in quality, as a thesis for the degree of Master of Science.

Prof. Dr. M. Cemal Yalabık (Supervisor)

I certify that I have read this thesis and that in my opinion it is fully adequate, in scope and in quality, as a thesis for the degree of Master of Science.

Prof. Dr. Bilal Tanatar

I certify that I have read this thesis and that in my opinion it is fully adequate, in scope and in quality, as a thesis for the degree of Master of Science.

Prof.Dr. Metin Gürses

Approved for the Institute of Engineering and Science:

Prof. Dr. Mehmet B. Baray
Director of the Institute Engineering and Science

ABSTRACT

MEAN-FIELD RENORMALIZATION GROUP THEORY OF THE t-J MODEL

Cengiz Şen
M.S. in Physics
Supervisor: Prof. Dr. M. Cemal Yalabık
July, 2002

The quantum nature of the high temperature superconductivity models makes analytical approaches to these systems almost impossible to implement. In this thesis, a computational study of the one and two dimensional $t - J$ models that combines mean-field treatments with renormalization group techniques will be presented. This allows one to deal with the noncommutations of the operators at two consecutive sites of the lattices on which these models are defined. The resulting phase diagram for the 1D $t - J$ model reveals an antiferromagnetic ground state, which may, upon doping with increasing temperature, show striped formation that is seen in the high-T_c cuprates. The qualitative features of the phase diagram of the 2D case is also presented, which reveals a phase transition between the disordered and antiferomagnetically ordered phases.

Keywords: high-temperature superconductivity, $t - J$ model, Hubbard model, renormalization group theory, mean-field theory, hard-spin mean-field theory.

ÖZET

$t - J$ MODELİNİN ORTALAMA ALAN RENORMALİZASYON GRUP TEORİSİ

Cengiz Şen
Fizik, Yüksek Lisans
Tez Yöneticisi: Prof. Dr. M. Cemal Yalabık
Temmuz, 2002

Yüksek sıcaklık süperiletkenliği modellerinin kuvantum doğası, bu sistemlere karşı analitik yaklaşımları neredeyse olanaksız kılmaktadır. Bu tezde, bir ve iki boyutlu $t - J$ modellerinin, ortalama alan yaklaşımlarıyla renormalizasyon grup tekniklerini birleştiren sayısal bir çalışması sunulacaktır. Bu, modellerin tanımlandığı örgünün iki ardışık bölgesindeki operatörlerin yer değiştirilememesini ele almayı mümkün kılmaktadır. Bir boyutlu $t - J$ modelinin ortaya çıkan faz diyagramı, artan sıcaklıkla katkılama ile antiferromagnetik bazal durumun yüksek-T_c materyallerinde görülen çizgili bir dönüşüm gösterebileceğini ortaya koymaktadır. İki boyutlu durumun faz diyagramının antiferromagnetik düzenli ve düzensiz fazlar arasındaki faz geçişini ortaya koyan kalitatif özellikleri de sunulmaktadır.

Anahtar kelimeler: yüksek sıcaklık süperiletkenliği, $t - J$ modeli, Hubbard modeli, renormalizasyon grup teorisi, ortalama-alan teorisi, sert-spin ortalama-alan teorisi.

Acknowledgement

I would like to express my gratitude to my supervisor Prof. Dr. M. Cemal Yalabık for his instructive comments and guidance in the preparation of this thesis. I am indebted to him so much, not only in academic issues but also because of his friendly attitude over the last two years.

My thanks also go to Prof. Dr. Bilal Tanatar and Prof. Dr. Metin Gürses for a critical reading of the manuscript and suggesting the necessary corrections.

I also would like to thank to M.S. Özge Günaydın for her encouraging support. It is my pleasure to dedicate this and all forthcoming works to my family.

Contents

List of Figures

List of Tables

Chapter 1

INTRODUCTION

The announcement of the first high-T_c cuprate in 1986 by J. G. Bednorz and K. A. Muller[1] at a temperature of 30 K opened a new era in superconductivity. Although superconductivity is known since 1913 from a series of experiments performed by Heike Kamerlingh Onnes[2], the new superconductors were quite different than the old ones, mainly because these superconductors were oxides rather than metals. At first the results seemed unexpected, but the confirmation later came with even higher transition temperatures by Takagi *et. al.*[3] in 1987. This work made it possible to use inexpensive and easily available nitrogen instead of expensive and complex helium cooling systems in order to achieve superconductivity. Afterwards, the transition temperature has risen dramatically, examples are $YBa_2Cu_3O_7$ with T_c=94 K (the first superconductor having T_c greater than the boiling temperature of nitrogen, T=77,4K) (1987), a mercury based copper oxide material with T_c=133 K (1993), again a mercury based copper oxide with T_c=166 K (1996).

Theoretical studies concerning high temperature superconductivity have gained acceleration over the past years with the development of new ideas as well as the exponential growth of the computing technology. However, the mechanism of superconductivity in these materials remains mysterious in the sense that the conventional BCS theory of superconductivity[4] cannot be applied to these materials. The reason for that lies behind the fact that in the BCS theory,

the coherence length associated with the average size of a Cooper pair is large ($\sim$500Å–10000Å) with respect to that of high-T_c compounds ($\sim$12Å–15Å). Thus, for high-T_c cuprates, the application of standard mean field techniques may not reveal the real physics of the problem. However, the central idea of the BCS theory, which is the pairing of electrons, is still used to find out some properties of high-T_c materials.

In the search for a Hamiltonian to describe the behavior of these materials, the one-[5] and three-band Hubbard models[6, 7, 8] and the t-J model[9] were proposed. Although these models are results of great simplifications, they are now in the center of theoretical studies. The theories that combine the pairing ideas with strong antiferromagnetic correlations seen in the cuprates contain spin-bag type theories[10, 11, 12], antiferromagnetic Fermi-liquid theories[13], and $d_{x^2-y^2}$ theories [14, 15]. In the spin-bag type theories, superconductivity is explained based on the observation that in these materials there exists an antiferromagnetic spin ordering over distances large compared to lattice spacing. This spin correlation produces an electronic pseudogap Δ_{SDW} which is locally suppressed by the addition of a hole. This suppression in turn forms a bag inside which the hole is self-consistently trapped. Then these holes are attracted by sharing a common bag, and this pairing interaction $V_{\mathbf{k}-\mathbf{k}'}$ leads to a superconducting energy gap Δ_{SC} which is nodeless over the Fermi surface. In ref.[13], the antiferromagnetic correlation length of 2,5 lattice constants is found for a phenomenological model of a one-component system of antiferromagnetically correlated spins. It is shown that all of the available normal state NMR and NQR measurements in the $YBa_2Cu_3O_7$ are quantitatively well-explained by this model. The calculations based on the pairing mechanism that involve antiferromagnetic spin fluctuations support the proposal that high-T_c superconductors possess a $d_{x^2-y^2}$-type symmetry in the superconducting state, as opposed to s-wave symmetry seen in normal superconductors. It has been shown that[15], this highly-anisotropic state is consistent with NMR measurements. A typical phase diagram for high-T_c materials is shown in Figure 1.1. The antiferromagnetic phase dominates near half-filling, and is superseded by superconductivity (SC) at higher dopings, often by way of spin glass (SG) phase. At extreme overdoping, the material becomes a metal.

The underdoped normal state exhibits many anomalous properties which are indicative of its non-Fermi Liquid nature.

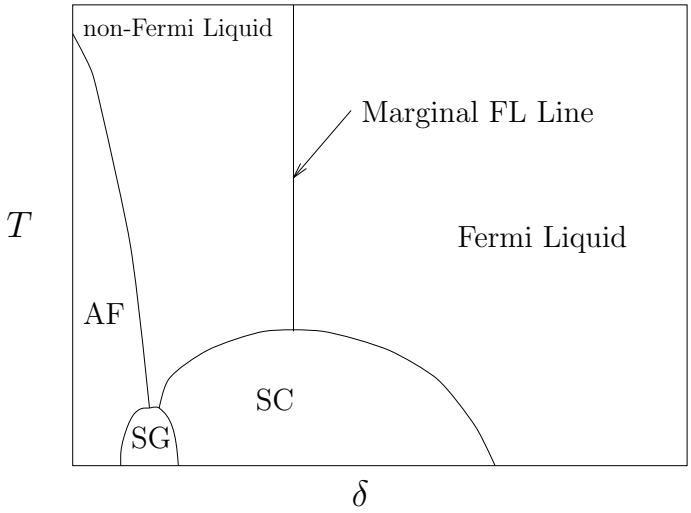

Figure 1.1: A typical phase diagram for high-temperature superconductors. T is the temperature, δ is the doping.

Theories that do not use the pairing ideas treat the excitations as spinons and holons[16]. Spinons have zero charge and spin 1/2, whereas holons have the charge e and spin 0. In this direction the 1D Hubbard model has been discussed by Anderson[17]. Among the other approaches to the high-T_c superconductivity are anyon superconductivity[18, 19, 20], gauge theories[21], and marginal Fermi-Liquid theories[22]. In anyon superconductivity theories, it has been mentioned that a spinon carrying half-fermion statistics plausibly binds to any introduced hole and creates a spinless charged half-fermion composite. Then, two half-fermions can pair to make a boson, which is a good candidate for a superconducting condensate. It has also been shown that[20], these pairs are energetically favorable. A fluctuating gauge field scatters holes strongly and the superconductivity coincides with the onset of coherence among the holes[21]. It is claimed that[22] the normal state anomalies in the Cu-O high-T_c superconductors follow from the fact that there exists spinon and holon excitations with the absorptive part of the polarizability at low frequencies ω proportional to ω/T and constant otherwise. This hypothesis characterizes these materials in the normal state as marginal Fermi-liquids and leads to an attractive particle-particle interaction for superconductive pairing. Other approximations such as perturbative calculations

in bubble and ladder diagrams, as well as self-consistent ones (mainly mean-field-like) have results that are difficult to judge their results as to their closeness to the actual properties of the models[23].

Although all of the aforementioned approaches helped in many ways in understanding different aspects of these materials, the difficulty in the solutions of the $t-J$ and the Hubbard models prevents a clear-cut theory for high-temperature superconductivity. As yet, only one-dimensional cases of these models are fully understood[25, 26], which are not so interesting because of the 2D nature of the problem. However, even in 1D, Ogata *et. al.* showed that[26] there exist a region in the parameter space where superconducting correlations become dominant. The solution of Ref.[26] utilizes exact diagonalization and exact solutions at $J/t = 0$ and 2. It is shown that phase separation takes place above a critical value of J around $J_c = 2.5 - 3.5$ depending on the electron density. There is no phase separation in the 1D Hubbard model. The phase- separation in the 2D $t-J$ model is investigated using high-temperature series expansion by Putikka *et. al.* through tenth order[27]. It was shown that the phase separation is quite different than the 1D case, since in one-dimension the phase-separation line is in the relatively narrow range between $J/t = 2.7$ as $n \to 0$ and $J/t = 3.5$ at half-filling, whereas in 2D it extends from $J/t = 3.8$ as $n \to 0$ to $J/t = 1.2$ near half-filling. Also the slope of the phase-separation line in the 1D case is positive, whereas it is negative in the 2D case[27, 28]. For a complete list of references regarding the early times of high-temperature superconductivity theories, refer to the review article by Dagotto[23].

More recent approaches to the $t-J$ model focus on the configuration of electrons and holes in the superconducting state. One possible candidate is the so-called striped phase, where electrons and holes arrange themselves in such a way that the configuration goes as two electrons one with spin up and the other with spin down followed by two holes. This state has been examined by many groups with numerous techniques, both analytically as well as numerically. Among them are density matrix renormalization group (DMRG) studies[29, 30], exact diagonalization techniques[31], and computational studies[32, 33]. In the density matrix renormalization group study of the 2D $t-J$ model, a striped

phase is found at a hole doping of $x = 1/8$ on clusters as large as 19×8[29]. At the same hole doping, it was shown that[31] the low-energy states of the 2D $t-J$ model are uniform, whereas the excited states with charge density wave structures could be interpreted as striped phases. Computational studies indicate that[32] the elementary stripe "building block" resembles the properties of *one* hole at small J/t, with robust AF correlations across the hole induced by the local tendency of the charge to separate from the spin. Thus, it is argued that the seed of half-doped stripes already exists in the unusual properties of the insulating compounds.

In the next chapter, the models of high-T_c superconductivity and the hard-spin mean-field theory are discussed, the latter of which constitutes an important aspect of the approximation that is used in this thesis. Due to the quantum nature of the problem, one should be very careful in handling the models that are mentioned above. The hamiltonians of these models consists of operators that does not commute at the two consecutive sites of the lattice on which all these hamiltonians are defined. This clearly makes a conventional renormalization group calculation questionable. Thus, in the third chapter, a way to overcome this difficulty is presented with an application to the 1D $t-J$ model. This method combines the hard-spin mean-field theory with the block-spin transformation of renormalization theory, yielding a finite temperature phase diagram for the 1D $t-J$ model. In the fourth chapter, a similar approach is applied to the 2D case, this time with mean-field theory instead of the hard-spin mean-field theory, due to some limitations discussed in the text. In the last chapter, we conclude with the results.

Chapter 2

THEORETICAL BACKGROUND

In this chapter, theoretical background that is necessary for the following chapters will be elucidated. The chapter starts with the Heisenberg model and continues with the Hubbard model and the $t-J$ model. The reduction of the Hubbard model to the one-band $t-J$ model in the strong coupling regime will also be presented. Mean-field theory and renormalization group theory are examples of general theories about which the reader can find information easily[39]. For this reason, this chapter contents with the hard-spin mean-field theory and closes with an application to the 2D Ising model.

2.1 Heisenberg Model

Strong antiferromagnetic correlations are dominant in high-T_c cuprates. It is this feature of these materials that makes necessary to study first the spin-spin interaction term, i.e. the Heisenberg term, before going on with the Hubbard model and the $t-J$ model. Indeed, both of these models include the Heisenberg term. The Heisenberg hamiltonian put spins on a square lattice and lets the spins interact with a vector interaction[24]. In the most general form, the Heisenberg

model is defined as:

$$\begin{aligned} H &= \sum_{\langle ij \rangle} J_{ij} \mathbf{S}_i \cdot \mathbf{S}_j \\ &= \sum_{\langle ij \rangle} J_{ij} (S_{ix} S_{jx} + S_{iy} S_{jy} + S_{iz} S_{jz}). \end{aligned} \tag{2.1}$$

where J_{ij} is the interaction constant between the spin at the ith site and the spin at the jth site. In general the summation is taken over all sites $\langle ij \rangle$, but for simplicity, one takes into account only the nearest neighbor interaction and treats the system as an isotropic one. In this case J is a constant and can be taken outside the summation:

$$H = J \sum_{\langle ij \rangle} \mathbf{S}_i \cdot \mathbf{S}_j \tag{2.2}$$

In this convention, J is positive for antiferromagnetic interaction and negative for ferromagnetic interaction. Note that Heisenberg model reduces to the Ising model in the absence of S_x and S_y terms, and reduces to the XY model in the absence of the S_z term. It is possible to write this hamiltonian in many ways, e.g. in the ladder representation, defining:

$$S_{ix} = \frac{1}{2}(S_{i+} + S_{i-}), \quad S_{iy} = \frac{-i}{2}(S_{i+} - S_{i-}), \tag{2.3}$$

it is possible to write the Heisenberg hamiltonian as:

$$H = \frac{J}{2} \sum_{\langle ij \rangle} (S_{i+} S_{j-} + S_{i-} S_{j+} + 2 S_{iz} S_{jz}) \tag{2.4}$$

The operator(s) S_{i+} (S_{i-}) can be thought of as creating (destroying) a spin up (down) electron at site i. The Heisenberg model is often solved for spin greater than one-half or for coupling between spins which may be further neighbors. Here the word *solve* means "approximately solve", since it has not been solved exactly, except in one dimension[25].

2.2 Hubbard Model

2.2.1 Three-Band Model

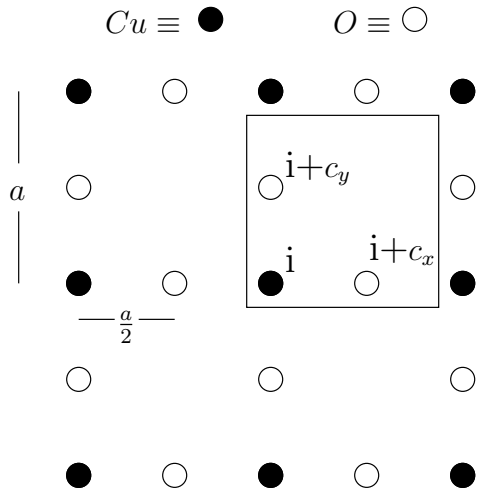

Figure 2.1: 2D CuO_2 lattice

Emery first suggested that[6] the electronic structure of the CuO_2 planes can be described by a Hubbard Hamiltonian on a 2D-lattice having one Cu site and two O sites per unit cell shown in Figure 2.1. A single $3d_{x^2-y^2}$ orbital in each Cu site as to become hybridized with each of the four $2p_x, 2p_y$ orbitals of the surrounding O sites pointing toward the i-site, as shown in Figure 2.2. In addition, a strong Coulomb repulsion term is present when two electrons happen to be both in the 3d orbital at the same site i. A hamiltonian describing the above interactions is of the form:

$$\begin{aligned} H &= \sum_{i\sigma} \epsilon_d d^\dagger_{i\sigma} d_{i\sigma} + U \sum_i n_{i\uparrow} n_{i\downarrow} + \sum_{\mu\sigma} \sum_{\alpha} \epsilon_p p^{\alpha\dagger}_{\mu\sigma} p^{\alpha}_{\mu\sigma} \\ &+ \sum_{i\sigma} \sum_{\mu_i} (V_{i\mu} d^\dagger_{i\sigma} p_{\mu_i\sigma} + h.c.). \end{aligned} \tag{2.5}$$

where the Latin indices label sites on an arbitrary lattice, $\sigma = \uparrow, \downarrow$ is a spin index (for spin-1/2 fermions) and i and μ denote, respectively, the Cu sites and the O sites; $d^\dagger_{i\sigma}, p^{\alpha\dagger}_{\mu_i\sigma}$ create electrons with spin σ in the $Cu(3d_{x^2-y^2})$ and $O(2p_x)$ or $O(2p_y)$ orbitals of energies ϵ_d and ϵ_p. In Equation 2.5, the sum over $\mu_i = i \pm c_x$;

$\mu_i = i \pm c_y$ runs over the four $O-$sites around the $Cu-$site i and, according to the hybridization scheme of Figure 2.2, it is understood that the $p_{\mu_i\sigma}$'s indicate $p^x_{\mu_i\sigma}$ and $p^y_{\mu_i\sigma}$ for $\mu_i = i \pm c_x$ and $\mu_i = i \pm c_y$ respectively.

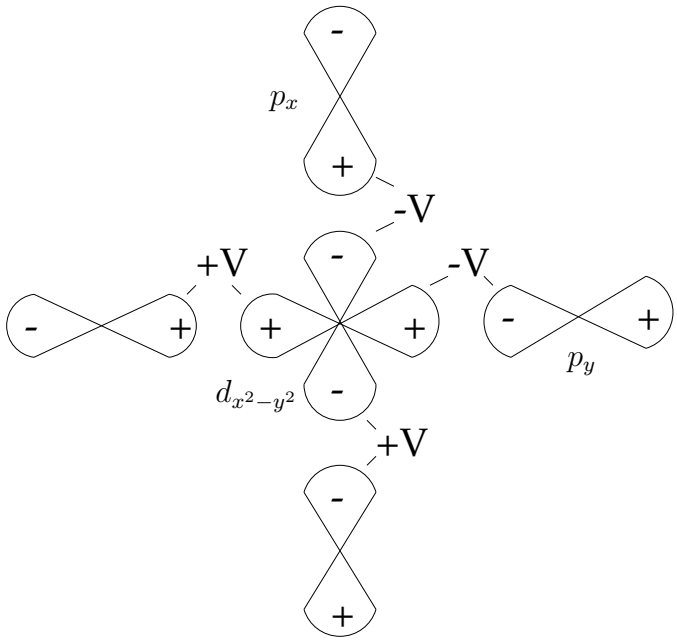

Figure 2.2: Hybridization scheme between $Cu - 3d_{x^2-y^2}$ and $O - p_x, p_y$ orbitals

The hybridization matrix element $V_{i\mu}$ is assumed to be proportional to the overlap of the corresponding $3d$ and $2p$ orbitals and has then the form

$$V_{i\mu} = (-1)^{\alpha_{i\mu}} V \tag{2.6}$$

with

$$\alpha_{i\mu} = \begin{cases} 1 & \text{for } \mu_i = i + c_x; \mu_i = i + c_y; \\ 0 & \text{for } \mu_i = i - c_x; \mu_i = i - c_y. \end{cases} \tag{2.7}$$

2.2.2 One-Band Model

A more simpler, one-band, version of the Hubbard model is defined by the many-body hamiltonian:

$$H = -\sum_{ij}\sum_{\sigma} t_{ij} c^{\dagger}_{i\sigma} c_{j\sigma} + \frac{1}{2}\sum_{ijkl}\sum_{\sigma\sigma'} \langle ij|v|kl\rangle c^{\dagger}_{i\sigma} c^{\dagger}_{j\sigma'} c_{l\sigma'} c_{k\sigma} \tag{2.8}$$

where the $c_{i\sigma}$ and $c^{\dagger}_{i\sigma}$ are electron annihilation and creation operators, t_{ij} is the hopping integral between the sites i and j, and v is the two-body Coulomb potential. For simplicity, one considers only the nearest neighbor (n.n.) hopping:

$$t_{ij} = \begin{cases} t & (i,j) = \text{n.n.} \\ 0 & \text{otherwise} \end{cases} \tag{2.9}$$

and screened interactions:

$$\langle ij|v|kl\rangle = \begin{cases} U & i = j = k = l \\ 0 & \text{otherwise} \end{cases} \tag{2.10}$$

For a single band, this implies $\sigma' = -\sigma \equiv \bar{\sigma}$, and the simplest version of the model becomes:

$$H = -t\sum_{\langle ij\rangle}\sum_{\sigma} c^{\dagger}_{i\sigma} c_{i\sigma} + U\sum_{i} n_{i\uparrow} n_{i\downarrow}, \tag{2.11}$$

where $n_{i\sigma} = c^{\dagger}_{i\sigma} c_{i\sigma}$ and $\langle ij\rangle$ denotes a sum over n.n. ordered pairs.

2.3 $t - J$ Model

2.3.1 Three-Band Model

Due to very strong $Cu - O$ bonds on the planes, the basic assumption in writing a hamiltonian to describe the high-T_c materials is to restrict the consideration in electrons moving on the CuO_2 planes. The Cu^{2+} ions have nine electrons in the $5d$ orbitals, while O^{2-} ions have their $3p$ orbitals occupied. This can further

be simplified by taking into account that every Cu atom is surrounded by a O atom as shown in Figure 2.1. The copper and oxygen orbitals can be shown to separate, and the state with highest energy is a $d_{x^2-y^2}$ wave carrying the missing electron which gives the ion its spin-1/2. This is schematically illustrated in Figure 2.3. Thus, with one hole per unit cell (i.e. in the absence of doping), the planes can be described by a model of mostly localized spin-1/2 states that gives these materials their antiferromagnetic character. The other energy levels are occupied, and as a first order approximation, they can be neglected. It has

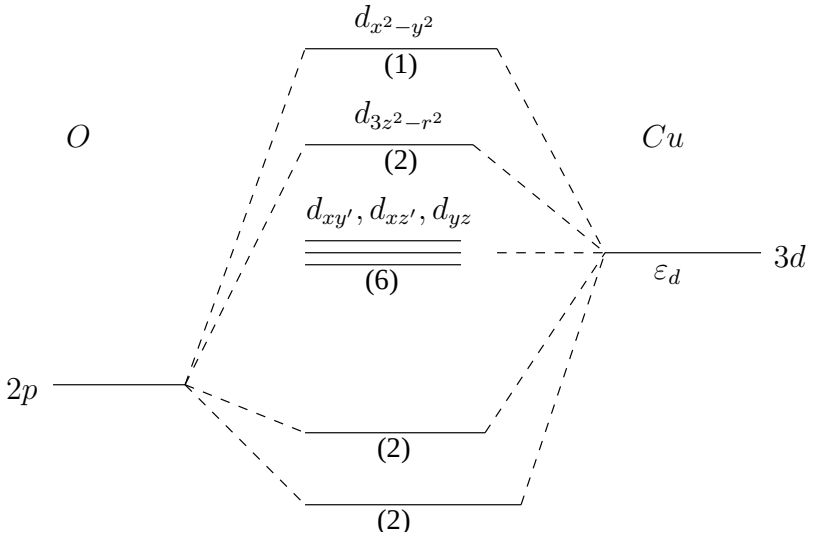

Figure 2.3: Formation of bonding between a Cu^{2+} and two O^{2-} ions. Only the d electrons of Cu and the p_x and p_y orbitals of the oxygens are considered. The numbers in the parentheses are occupations of the levels in the undoped system[23].

been mentioned before that high-T_c compounds are indeed insulators with strong antiferromagnetic correlations in the presence of doping. In order for this to be preserved, upon doping, the double occupancy of the $d_{x^2-y^2}$ orbital must be energetically unfavored, hence giving the material its antiferromagnetic character. Then, the three band model can be written as[6, 7, 8] (with the vacuum defined

as filled Cud^{10} and Op^6 states):

$$\begin{aligned} H &= -t_{pd}\sum_{\langle ij\rangle}(p_j^\dagger d_i + p_j d_i^\dagger) - t_{pp}\sum_{\langle jj'\rangle}(p_j^\dagger p_{j'} + p_j p_{j'}^\dagger) + \epsilon_d\sum_i n_i^d + \epsilon_p\sum_j n_j^p \\ &+ U_d\sum_i n_{i\uparrow}^d n_{i\downarrow}^d + U_p\sum_j n_{j\uparrow}^p n_{j\downarrow}^p + U_{dp}\sum_{\langle ij\rangle} n_i^d n_j^p. \end{aligned} \tag{2.12}$$

Indeed, this is an extended Hubbard model, where p_j's are fermionic operators that destroy holes at the oxygen sites labeled j, d_i's the similar operators for the copper sites labeled i. The terms t_{pd} and t_{pp} correspond to the hopping amplitudes between $Cu-O$ and $O-O$, respectively. U_d and U_p are Columbic repulsions when two electrons happen to be at same d and p orbitals and U_{pd} is the Columbic repulsion between a Cu site and a O site. The $O-O$ hopping term t_{pp} and the repulsion term U_p are introduced for completeness and they can be neglected in reduction to the one-band model. In the strong coupling limit this model reduces to the Heisenberg model with a superexchange antiferromagnetic coupling[8]. Typical values of the parameters in the Hamiltonian is given in Table 2.1.

$\epsilon_p - \epsilon_d$	t_{pd}	t_{pp}	U_d	U_p	U_{pd}
3.6	1.3	0.65	10.5	4	1.2

Table 2.1: The estimates for the values in the three-band $t-J$ model in eV's.

2.3.2 One-Band Model

Zhang and Rice introduced a single-band hamiltonian in order to describe the superconducting CuO_2 planes[9]. Their main reasoning is based on hybridization that strongly binds a hole on each square of O atoms to the central Cu^{2+} ion to form a local singlet. Then, this singlet moves through the lattice of Cu^{2+} ions in a similar way as a hole in the one-band effective hamiltonian. Here, it is important to make the distinction between holes and vacancies. A vacancy is a missing oxygen atom, while a hole is an oxygen atom with charge -1 instead of

-2[34]. With the removal of the terms introduced for completeness and the term corresponding to the Columbic repulsion between a Cu site and a O site, the hamiltonian in Equation 2.19 becomes:

$$H = -t_{pd} \sum_{\langle ij \rangle} (p_j^\dagger d_i + p_j d_i^\dagger) + \epsilon_d \sum_i n_i^d + \epsilon_p \sum_j n_j^p + U_d \sum_i n_{i\uparrow}^d n_{i\downarrow}^d. \tag{2.13}$$

Consider the case when the atomic energy of the Cu holes $\epsilon = 0$ and $\epsilon > 0$. The hybridization matrix, t_{pd}, is assumed to be proportional to the wave-function overlap of the Cu and O holes. It is also assumed to be constant and taken outside of the summation. Taking into account of the phase factor, and assuming the $Cu - Cu$ distance is the lattice constant, one can write it as:

$$-t_{pd} = (-1)^{n_{t,p}} t_0, \tag{2.14}$$

where t_0 is the amplitude of the hybridization, $n_{p,d} = 2$ if $l = i - \frac{1}{2}\hat{x}$ or $l = i - \frac{1}{2}\hat{y}$, and $n_{p,d} = 1$ if $l = i + \frac{1}{2}\hat{x}$ or $l = i + \frac{1}{2}\hat{y}$. In the absence of doping, the La_2CuO_4 has 1 hole per Cu. At $t_0 = 0$, all the Cu sites are singly occupied, and all the O sites are empty in the hole representation. When t_0 is small, then the virtual hopping processes involving the doubly occupied Cu hole states produces a superexchange antiferromagnetic interaction between neighboring Cu sites, and the model is well described by the Heisenberg model:

$$H = J \sum_{\langle ij \rangle} \mathbf{S}_i \cdot \mathbf{S}_j, \quad J = \frac{4t_0^4}{\epsilon_p^2} (\frac{1}{U} + \frac{1}{2\epsilon_p}). \tag{2.15}$$

Here the summation is taken over nearest-neighboring sites, and $\mathbf{S}$'s are spin-$\frac{1}{2}$ operators. Consider the copper ion surrounded by four oxygen hole states shown in Figure 2.2. The states of the holes can be either symmetric or antisymmetric with respect to the central Cu ion. When combined with the Cu hole, these states form singlet and triplet states. To the second order in perturbation theory about the atomic limit, the energy of the spin singlet state has the lowest energy[9], and hence it is possible to work in the subspace of the spin singlet state, without changing the physics of the problem. This effectively corresponds to replacing the hole originally located at the oxygen by a spin singlet state centered at the

Cu-site. In turn, the model is equivalent to electrons and spinless holes moving on a 2D square lattice shown in Figure 2.4.

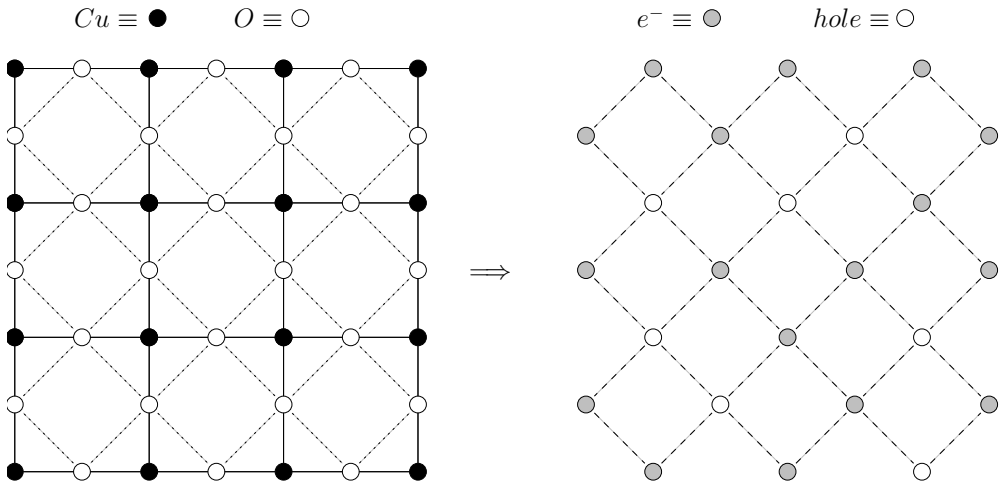

Figure 2.4: Reduction of the three-band model to the one-band $t - J$ Model.

The one-band $t - J$ model can now be written as:

$$\begin{aligned} H &= -t \sum_{\langle ij \rangle, \sigma} [(1 - n_{i-\sigma}) c^{\dagger}_{i\sigma} c_{j\sigma} (1 - n_{j-\sigma}) + (1 - n_{i-\sigma}) c_{i\sigma} c^{\dagger}_{j\sigma} (1 - n_{j-\sigma})] \\ &+ J \sum_{\langle ij \rangle} [\mathbf{S}_i \cdot \mathbf{S}_j - \frac{1}{4} n_i n_j]. \end{aligned} \tag{2.16}$$

where $\mathbf{S}_i$ are spin-1/2 operators at the sites i of the 2D lattice, and J is the antiferromagnetic interaction between the nearest neighbors sites. The hopping t term corresponds to the kinetic energy that allows the movement of the electrons in the lattice. The doubly occupied sites are not allowed and are projected out by the operators $(1 - n_{i-\sigma})$. With this definition, one considers only three possible states per site, i.e. an electron with spin up or down or a hole. It is clear that in the absence of doping, i.e. $t = 0$, the model reduces to the Heisenberg model of interacting fermions in a 2D lattice.

It has to be mentioned that the reduction of the three-band model to the single-band model is still controversial and in the past it has been a subject of debate[35, 36, 37]. There is also another version of the $t - J$ model, the so-called

extended $t-J$ model which is defined by:

$$\begin{aligned} H &= t\sum_{\langle ij\rangle,\sigma}(c^{\dagger}_{i\sigma}c_{j\sigma}+c_{i\sigma}c^{\dagger}_{j\sigma})+t'\sum_{\langle ik\rangle,\sigma}(c^{\dagger}_{i\sigma}c_{k\sigma}+c_{i\sigma}c^{\dagger}_{k\sigma}) \\ &+ J\sum_{\langle ij\rangle}[\mathbf{S}_i\cdot\mathbf{S}_j-\frac{1}{4}n_in_j]. \end{aligned} \tag{2.17}$$

where the t' term is introduced to include the next-nearest neighbor hoppings. Again, it is understood that the doubly-occupied sites are not allowed. Although the extension can be generalized, in what follows, we shall assume that $t-J$ model of the Equation 2.23 can be used to describe the cuprates, and the higher order terms are small enough that they can be neglected.

2.4 Strong Coupling Limit of the One Band Hubbard Model

The Hubbard model is mainly studied in the strong coupling limit in the high-temperature superconductivity community. However, in this limit, this model reduces to the $t-J$ model as will be shown below. Hence, one can restrict himself to the $t-J$ model only.

Consider the one-band Hubbard model written as (this discussion follows that of Ref.[40]):

$$H = H_0 + V, \tag{2.18}$$

where H_0 is the hopping term and $V = U\sum_i n_{i\uparrow}n_{i\downarrow}$. Let $\mathcal{H}_n$ be the eigenspace of V with exactly n doubly occupied sites, corresponding therefore to the eigenvalue $E_n = nU$. The projectors $\mathcal{P}_n$ onto $\mathcal{H}_n$ can be generated by expanding:

$$\begin{aligned} \Pi(x) &= \prod_{i=1}^{N}[1-(1-x)n_{i\uparrow}n_{i\downarrow}] \\ &= \sum_{n=0}^{N}x^n\mathcal{P}_n, \end{aligned} \tag{2.19}$$

where $0 \leq x \leq 1$ and N is the number of sites in the lattice. In particular, the Gutzwiller projector which is defined as:

$$\mathcal{P}_0 = \prod_{i=1}^{N}(1 - n_{i\uparrow}n_{i\downarrow}) \tag{2.20}$$

selects the subspace containing no doubly-occupied sites at all, i.e. $n_i \leq 1$ as an operator inequality. One can as well define operator projecting onto the subspace containing at least one doubly-occupied site:

$$\mathcal{P}_\alpha \equiv \sum_{n\geq 0} \mathcal{P}_n. \tag{2.21}$$

Clearly, $\mathcal{P}_0 + \mathcal{P}_\alpha = \hat{1}$. Using the decomposition of identity, one can write:

$$H_0 \equiv \mathcal{P}_0 H_0 \mathcal{P}_0 + \mathcal{P}_\alpha H_0 \mathcal{P}_\alpha + \mathcal{P}_0 H_0 \mathcal{P}_\alpha + \mathcal{P}_\alpha H_0 \mathcal{P}_0, \tag{2.22}$$

and

$$V \equiv \mathcal{P}_\alpha V \mathcal{P}_\alpha. \tag{2.23}$$

It is trivial to check that: $\mathcal{P}_0 H_0 \mathcal{P}_\alpha = \mathcal{P}_0 H_0 \mathcal{P}_1$ and $\mathcal{P}_\alpha H_0 \mathcal{P}_\alpha = \mathcal{P}_1 H_0 \mathcal{P}_0$. Using the identity $c_{i\sigma} \equiv c_{i\sigma}[(1 - n_{i\bar{\sigma}}) + n_{i\bar{\sigma}}]$, one can write H_0 as[38]:

$$H_0 \equiv T_h + T_d + T_{mix}, \tag{2.24}$$

where:

$$T_h = -t \sum_{\langle ij\rangle,\sigma} (1 - n_{i\bar{\sigma}}) c^\dagger_{i\sigma} c_{j\sigma} (1 - n_{j\bar{\sigma}}); \quad \bar{\sigma} = -\sigma \tag{2.25}$$

$$T_d = -t \sum_{\langle ij\rangle,\sigma} n_{i\bar{\sigma}} c^\dagger_{i\sigma} c_{j\sigma} n_{j\bar{\sigma}} \tag{2.26}$$

$$T_{mix} = -t \sum_{\langle ij\rangle,\sigma} \{n_{i\bar{\sigma}} c^\dagger_{i\sigma} c_{j\sigma} (1 - n_{j\bar{\sigma}}) + n_{i\bar{\sigma}} c_{i\sigma} c^\dagger_{j\sigma} (1 - n_{j\bar{\sigma}})\}. \tag{2.27}$$

With these definitions of the terms in the one-band Hubbard model, we can write:

$$\begin{aligned} H &= \tilde{H}_0 + H_\alpha, \quad \text{where:} && (2.28)\\ \tilde{H}_0 &= \mathcal{P}_0 H_0 \mathcal{P}_0 + \mathcal{P}_\alpha H_0 \mathcal{P}_\alpha + V \quad \text{(diagonal term)}, && (2.29)\\ H_\alpha &= \mathcal{P}_0 H_0 \mathcal{P}_\alpha + \mathcal{P}_\alpha H_0 \mathcal{P}_0 \quad \text{(off-diagonal term)}. && (2.30) \end{aligned}$$

In order to find a canonical transformation eliminating the effect of H_α to lowest order, i.e. such that the transformed hamiltonian satisfies $\mathcal{P}_0 H_{eff} \mathcal{P}_\alpha = 0$ to the required order, one can start with the formal definition:

$$H(\lambda) = \tilde{H}_0 + \lambda H_\alpha, \tag{2.31}$$

and seek a canonical transformation of the form:

$$\mathcal{U}(\lambda) = e^{i\lambda\mathcal{S}}; \quad \mathcal{S} = \mathcal{S}^\dagger, \tag{2.32}$$

where $\mathcal{S}$ has to be such that the transformed hamiltonian $H_{eff}(\lambda)$ obeys:

$$H_{eff} = e^{i\lambda\mathcal{S}} H(\lambda) e^{-i\lambda\mathcal{S}} = \tilde{H}_0 + \mathcal{O}(\lambda^2). \tag{2.33}$$

Expanding Equation 2.40 in terms of λ, one gets:

$$H_{eff}(\lambda) = \tilde{H}_0 + \lambda(H_\alpha + i[\mathcal{S}, \tilde{H}_0]) + \lambda^2 (i[\mathcal{S}, H_\alpha] + \frac{1}{2}[\mathcal{S}, [\tilde{H}_0, \mathcal{S}]]) + \mathcal{O}(\lambda^2), \tag{2.34}$$

where $\mathcal{S}$ is determined from:

$$[\tilde{H}_0, \mathcal{S}] + iH_\alpha = 0. \tag{2.35}$$

Hence, up to terms of order t^2 (setting $\lambda = 1$), one finds:

$$H_{eff} = \tilde{H}_0 + \frac{i}{2}[\mathcal{S}, H_\alpha]. \tag{2.36}$$

In the low-energy limit with doubly occupied states are projected out by the

Gutzwiller projector $\mathcal{P}_0$, the effective hamiltonian H_{eff} is given by[38]:

$$\begin{aligned} \mathcal{P}_0 H_{eff} \mathcal{P}_0 &= \mathcal{P}_0 \hat{H}_{eff} \mathcal{P}_0 \quad \text{with} \\ \hat{H}_{eff} &= T_h + H^{(1)} + H^{(2)}, \end{aligned} \tag{2.37}$$

where:

$$T_h = -t \sum_{\langle ij \rangle, \sigma} (1 - n_{i\bar{\sigma}}) c^{\dagger}_{i\sigma} c_{j\sigma} (1 - n_{j\bar{\sigma}}), \tag{2.38}$$

$$H^{(1)} = 2t^2 \sum_{\langle ij \rangle} \sum_{\tau\sigma} (1 - n_{i\bar{\sigma}}) c^{\dagger}_{i\sigma} c_{j\sigma} n_{j\bar{\sigma}} n_{j\bar{\tau}} c^{\dagger}_{j\tau} c_{i\tau} (1 - n_{i\bar{\tau}}), \tag{2.39}$$

$$H^{(2)} = t^2 \sum_{\langle ijl \rangle} \sum_{\tau\sigma} (1 - n_{i\bar{\sigma}}) c^{\dagger}_{i\sigma} c_{j\sigma} n_{j\bar{\sigma}} n_{j\bar{\tau}} c^{\dagger}_{j\tau} c_{l\tau} (1 - n_{l\bar{\tau}}) \tag{2.40}$$

and $\langle ij \rangle$ denote nearest neighbors, while i and l are nearest neighbors to j. Indeed, the second term suggest the extended $t - J$ model touched upon in the previous section. Neglecting the second term and rearranging the first two terms with the definitions made for the $\mathbf{S}$ operators in Section 2.1, one gets the one-band $t - J$ model:

$$\begin{aligned} H_{t-J} &= -t \sum_{\langle ij \rangle, \sigma} (1 - n_{i\bar{\sigma}}) c^{\dagger}_{i\sigma} c_{j\sigma} (1 - n_{j\bar{\sigma}}) \\ &+ J \sum_{\langle ij \rangle} \{ \mathbf{S}_i \cdot \mathbf{S}_j - \frac{1}{4} n_i n_j \} \end{aligned} \tag{2.41}$$

as the strong coupling limit of the one-band Hubbard model. Thus, instead of studying the strong coupling limit of the Hubbard model, one can safely deal with the $t - J$ model.

2.5 Hard-Spin Mean-Field Theory

In the conventional mean-field theory of spin systems, a spin feels the effective field produced by the magnetizations of the nearby spins. This is clearly not the case in reality, since a given spin should feel the effective field which is determined

by the full spins ($\sigma_i = \mp 1$) of its neighbors. Hard-spin mean-field theory is developed[41] in order to fully incorporate this fact and is shown to yield very satisfactory results for various models[41]. To illustrate the basics of the theory, consider the spin$-1/2$ ferromagnetic Ising model defined with the hamiltonian $H = -J\sum_{\langle ij\rangle} S_{iz}S_{jz} + h\sum_i S_{iz}$, where h is the external field. For simplicity, consider the case when $h = 0$. In the lattice shown in Figure 2.5, the real spin in

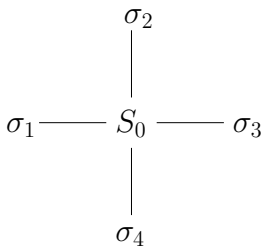

Figure 2.5: The spin configuration that is used in the hard-spin mean-field theory of the 2D Ising model.

the middle is coupled to hard-spins at the boundary denoted with Greek letters. Instead of the mean-field result for the magnetization $m = \tanh(J\sum_i m_i)$, hard-spin mean-field theory uses:

$$m = \tanh(J\sum_i \sigma_i), \tag{2.42}$$

where $\sigma_i = \mp 1$ with probability:

$$P_i(\sigma_i) = \frac{1 + \sigma_i m_i}{2}, \tag{2.43}$$

where $m_i = \langle S_{iz}\rangle$ is the local magnetization. However, in our case the interaction is isotropic and this gives $m_i = \langle S_0\rangle \equiv m$. The probability in Equation [2.43] is found by writing the most general form and then minimizing it with respect to the constraints $\sum_i P_i = 1$ and $\sum_i P_i\sigma_i = m$. The sum in Equation 2.42 is over all neighboring spins. The equation for the magnetization then becomes:

$$m = \sum_{\{\sigma_i\}}\prod_i \left(\frac{1 + \sigma_i m}{2}\right)\tanh(J\sum_i \sigma_i), \tag{2.44}$$

where the sum $\{\sigma_i\}$ is over all interacting neighbor spin configurations. The index i runs from 1 to 4 in the present case. This gives a self-consistent equation for the magnetization. A similar equation can be written for the partition function from which one can extract various information like entropy, free energy, etc. These equations are solved numerically for the magnetization and partition function. In Figure 2.6, the results for the magnetization and the free energy are summarized. It is seen that the critical temperature at which the spontaneous magnetization sets is $J_c = 3.226$. The conventional mean-field result for J_c is 0.25, whereas the exact result is 0.4407. Thus, even in such a simple case considered above, the hard-spin mean-field theory gives more correct results that the conventional approach where the effective field is determined by magnetizations instead of hard-spins.

The hard-spin mean-field theory is used in the renormalization group theory of the 1D $t - J$ model in the next chapter. However, because of computational difficulties, it is hard to implement it in the 2D case. This issue will be discussed further in the fourth chapter.

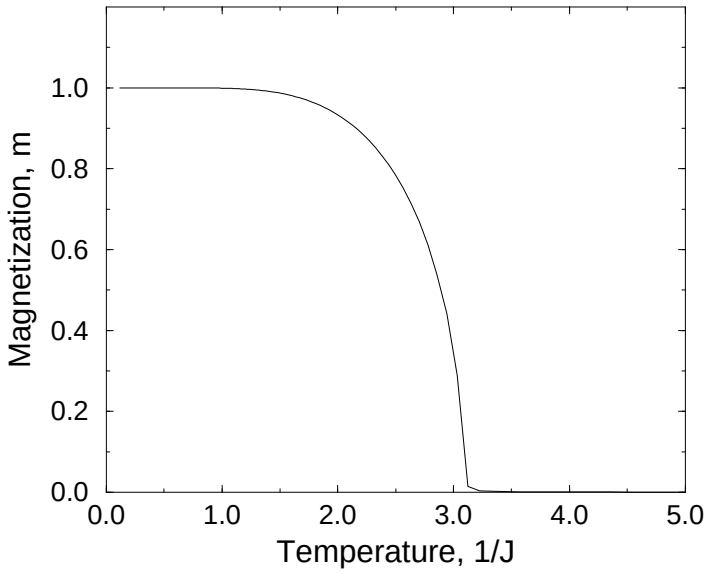

Figure 2.6: Magnetization (m) vs. temperature ($1/J$) for the 2D Ising model. $J_c = 0.3226$ to be compared with the exact value $J_c = 0.4407$.

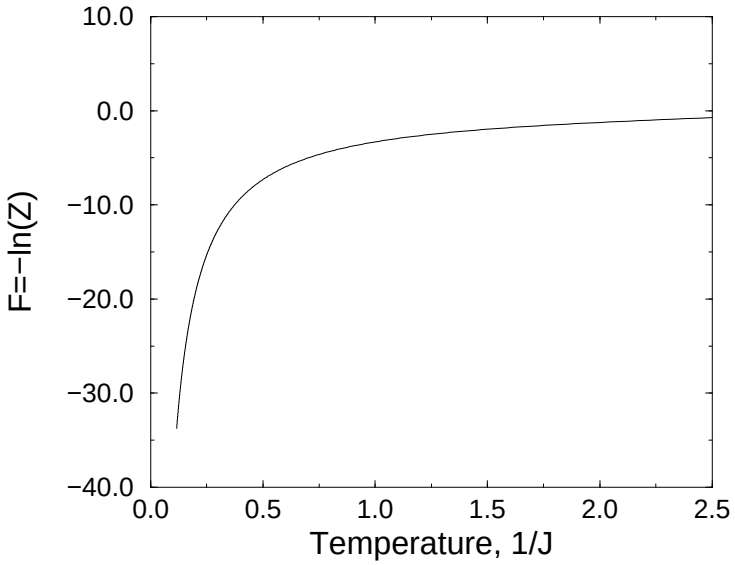

Figure 2.7: Free energy vs. temperature for the 2D Ising model calculated from the hard-spin mean-field approximation.

Chapter 3

ONE-DIMENSIONAL *t-J* MODEL

Although it is believed that high-temperature superconductivity is related to 2D CuO_2 planes, the 1D $t-J$ model also reveals some indications of superconducting correlations in the physically allowable region of the parameter space. The phase diagram of the 1D $t-J$ model is now widely understood [26], but the problem with the higher dimensions is still open. Ogata *et. al.*'s results show that phase separation takes place above a critical value of J around $J_c/t = 2.5 - 3.5$ depending on the electron density. They also mention that in the small J region the Tomonaga-Luttinger liquid theory holds and that the superconducting correlations become dominant between the exactly solvable case ($J/t = 2$) and phase separation. As Anderson claimed[16] 2D strongly correlated electronic systems could share some properties of 1D case. In this chapter, the results of a hard-spin mean-field theoretical renormalization group technique for the 1D $t-J$ is presented. We have found ordered and disordered phases separated by a phase separation line that is showed in the $1/V - t/V$ space. The character of the order is dependent upon the values of V/J and μ/J. The main program used in this study is given in Appendix A.1.

3.1 Motivation

The non-commutativity of the operators at the two consecutive sites of the lattice on which the $t-J$ hamiltonian is defined does not allow one to apply standard renormalization group techniques such as block-spin transformation and Migdal-Kadanoff renormalization group procedure. To illustrate this fact, consider 1D $t-J$ hamiltonian defined as:

$$-\beta H = \sum_i [-\beta H(i, i+1)], \tag{3.1}$$

with

$$H(i,j) = -t \sum_{\langle ij\rangle,\sigma} (c^\dagger_{i\sigma} c_{j\sigma} + c^\dagger_{j\sigma} c_{i\sigma}) - J \sum_{\langle ij\rangle} \mathbf{S}_i \cdot \mathbf{S}_j + V \sum_{\langle ij\rangle} n_i n_j + \mu \sum_i n_i \tag{3.2}$$

where t is the hopping amplitude, J is the spin-spin interaction constant ($+$ for antiferromagnetic, $-$ for ferromagnetic interaction), V stands for the Coulomb interaction, $c_{i\sigma}$ destroys an electron at site i with spin σ, the number operator $n_{i\sigma} = c^\dagger_{i\sigma} c_{i\sigma}$ and $\mathbf{S}_i$ are the electron density and spin operators at site i, and $n_i = n_{i\uparrow} + n_{i\downarrow}$. Note that the conventional $t-J$ hamiltonian is obtained when $V/J = 1/4$. Doubly occupied sites are not allowed and they can be thought of as projected out by a projection operator P defined as:

$$P = \Pi_i (1 - n_{i\downarrow} n_{i\uparrow}) \tag{3.3}$$

In what follows, the $+$ sign and $\uparrow$ as well as $-$ sign and $\downarrow$ will be used interchangeably. Now, suppose a renormalization group-transformation in which the renormalization is achieved by taking the trace over the even-numbered sites. In exact form this transformation can be written as[42]:

$$\begin{aligned} &\langle u_1 u_3 u_5 \dots | e^{-\beta' H'} | v_1 v_3 v_5 \dots \rangle \\ &\quad = \sum_{w_2 w_4 w_6 \dots} \langle u_1 w_2 u_3 w_4 u_5 w_6 \dots | e^{-\beta H} | v_1 w_2 v_3 w_4 v_5 w_6 \dots \rangle, \end{aligned} \tag{3.4}$$

where u_1, w_2, v_3 etc. represent the single-site states. Primes indicate the renormalized system. Although this renormalization conserves the partition function, it cannot be implemented due to the non-commutativity of the operators in the hamiltonian. An approximation of the form:

$$\begin{aligned}
\mathrm{Tr}_{\text{even states}} \exp(-\beta H) &= \mathrm{Tr}_{\text{even states}} \exp\left(\sum_i^{\text{even}} -\beta H(i-1,i) - \beta H(i,i+1)\right) \\
&\simeq \prod_i^{\text{even}} \mathrm{Tr}_{\text{even sites}} \exp(-\beta H(i-1,i) - \beta H(i,i+1)) \\
&= \prod_i^{\text{even}} \exp(-\beta' H'(i-1,i+1)) \\
&\simeq \exp\left(\sum_i^{\text{even}} -\beta' H'(i-1,i+1)\right) \\
&= \exp(-\beta' H'), \qquad (3.5)
\end{aligned}$$

has been applied to $t-J$ model[43] and gave no finite temperature phase transition in 1D. This approximation consists in ignoring, in two formally opposite directions, the noncommutations of operators between the two consecutive segments of the unnormalized system. Hence, an application of such an approximation is questionable. Instead, consider a three-site cluster that couples to the boundary with the Hartree-Fock approximated form of the interaction which is defined as:

$$AB = \langle A\rangle B + A\langle B\rangle - \langle A\rangle\langle B\rangle, \qquad (3.6)$$

and then continue with a block spin transformation, the details of which will be explained in the subsequent sections. This allows one to handle the problem taking into account the commutators between the operators at the boundary.[1] The approximation discussed here is a general one and can be applied to all lattice hamiltonians defined in arbitrary dimensions. In this chapter, it is applied to the 1D $t-J$ model and in the following chapter it is applied to the 2D $t-J$ model with minor differences from that of the 1D case.

[1]Indeed, this may be thought of as being equivalent to replacing the commutator of two operators by a c-number, instead of the zero value emerging from the approximation discussed in the text.

3.2 Hard-Spin Mean-Field Treatment of the Boundary

In order to evaluate the matrix elements of the $t-J$ hamiltonian, it is convenient to express both $\mathbf{S}_i$ and n_i in terms of creation and annihilation operators $c^\dagger_{i\sigma}$ and $c_{i\sigma}$. To do this one can define two other spin operators such that one of them first destroys an electron having spin $\downarrow$ at site i and then creates an electron with spin $\uparrow$ at the same site. Such an operator may be denoted as S_{i+} and in terms of the creation and annihilation operators it becomes $S_{i+} = c^\dagger_{i+}c_{i-}$. Similarly one can define the operator $S_{i-} = c^\dagger_{i-}c_{i+}$, i.e., destroying an electron having spin $\uparrow$ and creating a new one with spin $\downarrow$ at site i. Since

$$\mathbf{S}_i = S_{ix}\hat{\mathbf{x}} + S_{iy}\hat{\mathbf{y}} + S_{iz}\hat{\mathbf{z}}, \tag{3.7}$$

in the $\mathbf{S^2} - \mathbf{S_z}$ basis, one can define:

$$S_{ix} = \frac{1}{2}(S_{i+} + S_{i-}), \quad S_{iy} = \frac{-i}{2}(S_{i+} - S_{i-}), \quad S_{iz} = \frac{1}{2}(n_{i+} + n_{i-}). \tag{3.8}$$

It is seen that in this basis, the only contribution to the off-diagonal elements in the hamiltonian comes from the hopping term and the x- and y- components of the spin operator.

The operators defined above are used to generate the matrix elements of the $t-J$ hamiltonian for a three-site chain coupled to the boundaries with hard-spins that can take values $\sigma = -1$,0 and $+1$ with the probability evaluated as (see Appendix A.2):

$$P(\sigma, m, n) = (1-n) + \frac{1}{2}m\sigma + (\frac{3}{2}n - 1)\sigma^2, \tag{3.9}$$

where m is the magnetization and n is the occupation. Since there are 3 possible states attributed to one site, for a three-site chain, the hamiltonian is a 27 by 27 sparse matrix. The hamiltonian describing the internal dynamics of the three-site system is straightforward to evaluate, whereas the coupling to the outside requires special treatment, especially for the hopping term, t. Since the couplings are

achieved by hard-spins, a re-definition of the creation and annihilation operators at the boundary is needed in accordance with what value one attributes to these hard-spins. As an example, consider a hard spin with values $+1$ or -1. Now, if the neighboring site is occupied with an electron, the contribution from the hopping term to the hamiltonian is zero since the probability of hopping between these two sites is zero, no matter what spin values of these two sites have. In other words, the hopping is dependent upon whether one of the two neighboring sites is occupied and the other is not. For the spin-spin term, we can assume that only the z-component of the spins are coupled to each other, an approximation which becomes exact in the thermodynamic limit. The Coulomb term V and the chemical potential term μ is straightforward. The situation can be illustrated as:

$$\sigma_0 \text{——} S_1 \overline{\text{———}} S_2 \overline{\text{———}} S_3 \text{——} \sigma_4$$

Figure 3.1: Hard spins, σ's, interacting with the three site chain.

where $\overline{=}$ corresponds to internal dynamics of the spins and — corresponds to coupling of these "real" spins to the hard ones, σ. One can now write the "hoppingless" part of the hamiltonian as:

$$\begin{aligned} H &= -J(m_0 S_{1z} + \mathbf{S}_1 \cdot \mathbf{S}_2 + \mathbf{S}_2 \cdot \mathbf{S}_3 + S_{3z} m_4) \\ &+ V(\langle n_0 \rangle n_1 + n_1 n_2 + n_2 n_3 + n_3 \langle n_4 \rangle) \\ &+ \mu(\langle n_0 \rangle + n_1 + n_2 + n_3 + \langle n_4 \rangle), \end{aligned} \tag{3.10}$$

where m_0 and m_4 are the values that hard spins can take, and $\langle n_0 \rangle = m_0 m_0$ and $\langle n_4 \rangle = m_4 m_4$. In other words, $\langle n_i \rangle = 1$, when the ith site is occupied by a hard spin with $m_i = \mp 1$. The hopping part of the hamiltonian is plugged manually into the hamiltonian, considering the fact that it is zero when the two neighboring sites at the boundary are both occupied or unoccupied, and it is equal to $-t$ when one of them happens to be filled and the other is not.

In order to evaluate the partition function, $Z = \exp(-\beta H)$, one has to calculate the exponential of the hamiltonian matrix. For the case at hand, where the hamiltonian is a 27×27 matrix, this calculation has been done by a straight

Taylor series expansion of the exponential through 30th order. However, in 2D $t-J$ model where the hamiltonian matrix is a 243 $\times$ 243 matrix, the amount of computation time for the same exponentiation routine is significantly large, of the order of hours. A more efficient way, which is discussed in the next chapter, has to be implemented in this case.

3.3 Renormalization Group Procedure

The renormalization group procedure used here is the block spin transformation, where the coupling to the boundary is achieved via hard-spins mentioned in the previous section. Given the values for the five coupling constants (see below), namely $\mathbf{K} = (g, t, J, V, \mu)$, we are looking for the values of the renormalized or "primed" system, $\mathbf{K}' = (g', t', J', V', \mu')$. The details are as follows.

3.3.1 Block Spin Rule and States

The block spin transformation that will be used in the forward renormalization requires a definition of the majority rule for the block spins. This may be done in many ways provided that it preserves certain symmetries in the system. The system at hand has three possible states per site, an electron with spin up or down, and a hole. A convention is used: for a three-site chain, whenever the number of any of these states are equal to or greater than 2, then this block has this state as the block spin. If the number of all three is equal, and this number is 1 by definition, then this block has the value of the one that resides in the center of the chain. This definition of the majority rule treats all possible states on equal-footing, and preserves the symmetry that for the 27 possible configurations there are equal number of spin-up, spin-downs or holes, all nine. In Figure 3.2 this situation is schematically illustrated.

The $t-J$ model has four coupling constants in its hamiltonian, namely, $t, J, V,$

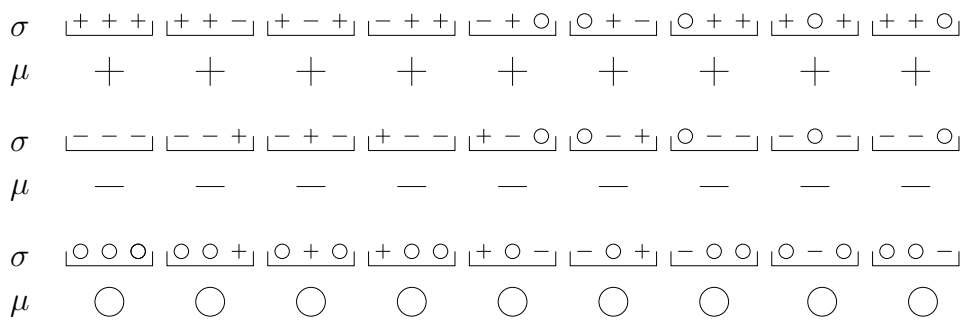

Figure 3.2: Block spin rule: σ's are the original spins, μ's are the block spins.

and μ. When renormalizing the system, an additional term representing the contribution to the free energy from the short wavelength degrees of freedom should be traced out. With this additional term, denoted as g, there are a total of five constants to be renormalized. This means that in order to construct the renormalization group equations, one has to choose at least five different states, all of which should give five linearly independent equations for the coupling constants. These states are chosen to be as in Figure 3.3. These states further preserves their forms under block spin renormalization group transformation, a feature that allows one to identify the low temperature fixed point. The state shown in Figure 3.3(e) is especially chosen, since it is believed to be the superconducting phase in the high temperature cuprates.

3.3.2 Forward Renormalization

The next step is to calculate the magnetizations, mean occupations and partition functions for the five different states defined in the previous section, by requiring all possible hard-spin configurations at the boundary. There are a total of nine such possibilities since each of the two hard spins can take three different values.

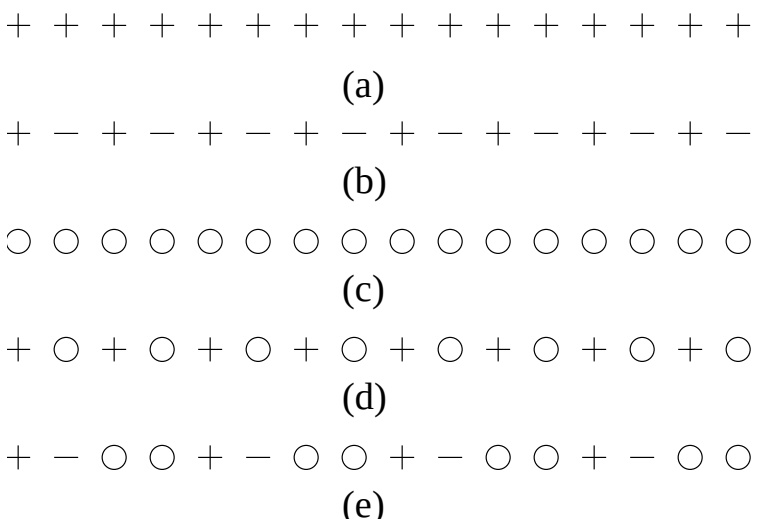

Figure 3.3: States that are used in the renormalization group procedure of the 1D $t-J$ model: (a) ferromagnetic state, (b) antiferromagnetic state, (c) empty state, (d) plus-hole state, (e) striped state.

These are calculated numerically from the equations:

$$m = \sum_{\sigma_0=0,\mp1} \sum_{\sigma_4=0,\mp1} P(\sigma_0, m, n) \times P(\sigma_4, m, n) \times m_\mu, \tag{3.11}$$

$$n = \sum_{\sigma_0=0,\mp1} \sum_{\sigma_4=0,\mp1} P(\sigma_0, m, n) \times P(\sigma_4, m, n) \times n_\mu, \tag{3.12}$$

$$Z = \sum_{\sigma_0=0,\mp1} \sum_{\sigma_4=0,\mp1} P(\sigma_0, m, n) \times P(\sigma_4, m, n) \times z_\mu. \tag{3.13}$$

Here, $P(\sigma, m, n)$ is the probability function defined in Equation 3.9, and m_μ, n_μ and z_μ are found by taking the trace of the partition function over the block spins $\mu = 0, \mp1$:

$$m_\mu = \mathrm{Tr}_\mu S_\mu e^{-\beta H}/z_\mu, \tag{3.14}$$

$$n_\mu = \mathrm{Tr}_\mu S_\mu^2 e^{-\beta H}/z_\mu, \quad \text{and} \tag{3.15}$$

$$z_\mu = \mathrm{Tr}_\mu e^{-\beta H}. \tag{3.16}$$

Of course, $m_1 = -m_{-1}$. Taking into account the effect of the last term in the Hartree-Fock approximation defined in Equation 3.6, the expression for z_μ becomes:

$$\begin{aligned} z_\mu &= \mathrm{Tr}_\mu \exp(-\beta H) \\ &\times \exp\left[t(\sqrt{1-n_0}\sqrt{n_{\mu,\mathrm{lb}}} + \sqrt{n_0}\sqrt{1-n_{\mu,\mathrm{lb}}})\right] \\ &\times \exp\left[t(\sqrt{1-n_4}\sqrt{n_{\mu,\mathrm{rb}}} + \sqrt{n_4}\sqrt{1-n_{\mu,\mathrm{rb}}})\right] \\ &\times \exp\left[\frac{1}{2}J(m_{\mu,\mathrm{lb}}m_0 + m_{\mu,\mathrm{rb}}m_4) - V(n_{\mu,\mathrm{lb}}n_0 + n_{\mu,\mathrm{rb}}n_4)\right], \end{aligned} \tag{3.17}$$

where lb and rb stand for left and right boundary, respectively, and $n_i = m_i^2$ for $i = 0$ and $i = 4$. The Equations $3.11 - 13$ implicitly give the value of the magnetization, mean occupation and the partition function for the states defined in Section [3.3.1]. For our purposes, the knowledge of the value of the partition function is sufficient for construction of renormalization group equations. The other two are given for reference purposes only.

3.3.3 Backward Renormalization

The renormalization group equations are given by the matrix equation:

$$\mathbf{R}(\mathbf{K}) = \mathbf{R}'(\mathbf{K}'), \tag{3.18}$$

where $\mathbf{R}$ and $\mathbf{R}'$ are 5×5 matrices, and $\mathbf{K}$ and $\mathbf{K}'$ are 5-dimensional vectors. This equation, in general, is nonlinear in $\mathbf{K}$ and $\mathbf{K}'$. The matrices are found by requiring that the renormalized and original systems conserve the *free energy per site*, that is:

$$\frac{1}{\beta}\ln(Z) = \frac{1}{\beta}\ln(e^{-\beta H}) = \frac{1}{\beta'}\ln(e^{-\beta' H'}) = \frac{1}{\beta'}\ln(Z'). \tag{3.19}$$

So, one has to calculate the free energy of the renormalized system, that is the system formed by the block spins, μ. This is indeed a difficult task, because it involves the solution of the original system. For example, for the ferromagnetic

state,

$$\langle + + + \cdots + + + | e^{\sum_{i,j} -\beta' H'(i,j)} | + + + \cdots + + + \rangle, \tag{3.20}$$

where the plus signs represent the block spins, should be calculated. Instead, we have used an approximation of the form:

$$\langle + + + \cdots + + + | e^{\sum_{i,j} -\beta' H'(i,j)} | + + + \cdots + + + \rangle \simeq \langle + + + | e^{-\beta' H'} | + + + \rangle, \tag{3.21}$$

where the only matrix element included in the sum is taken as the one between the ferromagnetic state of the three-site chain. The latter is used in the calculation of the free energies of the five different states. The Equation 3.8 is then solved numerically by the method of Gaussian elimination to give the renormalized coupling constants as functions of the original coupling constants. i.e.:

$$\mathbf{K}' = \mathbf{F}(\mathbf{K}). \tag{3.22}$$

3.3.4 Fixed Points

Fixed points satisfy the equation:

$$\mathbf{K}^* = \mathbf{F}(\mathbf{K}^*). \tag{3.23}$$

Six fixed points are found which are summarized in Table 3.1. The character of these fixed points are examined by the linearization of the Equation 3.22 around these fixed points. Eigenvalues of the linearization matrix are found as in Table 3.2. All of them has the eigenvalue ~ 3, corresponding to the term, g. The eigenvalues suggest that the fixed point labeled by the letter "B" is an attractive one and is a candidate of a high-temperature fixed point. The fixed point "C" has two eigenvalues with absolute values greater than one and two less than one. This may be an indicative of a critical fixed point. It is to be mentioned here that the fixed point "F" has complex conjugate eigenvalues, which are called the *irrelevant eigenvalues* in the renormalization group literature. The latter is seen in some random systems[39].

	g	t	J	V	μ
A	-1.0986	0.0000	0.0000	0.0000	0.0000
B	-7.3195	0.0119	0.0000	-0.0358	7.0002
C	-1.4691	1.6332	-0.0319	-1.2348	-0.5864
D	-0.2131	-0.0002	0.0000	0.0003	-2.4520
E	-3.8169	0.1308	-1.4047	4.2023	-6.5739
F	-12.3355	5.7689	0.9526	-7.9628	12.4538

Table 3.1: Fixed points that are found from the hard-spin mean-field renormalization group theory of the 1D $t-J$ model.

A	B	C	D	E	F
3.0000	3.0000	3.0018	2.9999	2.9917	3.0000
-0.0005	0.5048	-3.8476	0.0050	2.9409	-0.5468
0.0001	-0.0014	0.0485	-3.3404	-2.5039	$0.2766 + 0.1644i$
1.3340	0.0005	-2.0042	-5.5018	-0.0550	$0.2766 - 0.1644i$
0.1664	0.2389	-0.7649	-1.4109	-1.5126	-0.0384

Table 3.2: Eigenvalues of the linearization matrices corresponding to the fixed points for the 1D $t-J$ model.

3.4 Results and Discussion

By means of a repetitive iteration of randomly chosen points in some portion of the phase diagram, we have obtained a projection of the phase diagram in the $1/V - t/V$ space, for various values of V/J and μ/V. This is shown in Figure 3.4. We have found an ordered phase and a disordered phase separated by a separatrix that is seen in some random systems[39]. The points above the phase separation lines shown in Figure 3.4 eventually converge to the high temperature fixed point labeled by the letter "B". For the points lying below the lines, the behavior of V and μ show similar behaviors, V gets large negatively, whereas μ gets large positively. In this region, the character of the ordered phase reveals distinct properties depending upon how t and J converges. Below the solid line, the order seems to be of antiferromagnetic character, as t tends to zero J gets large (positive in our notation). That is, as μ gets large, the lattice is completely

filled and there is no space left for electrons to hop from one site to another. This fact is verified by the value of t getting smaller. The antiferromagnetic character is defined by the sign of J, which is positive in this case. Also, the calculated value of the partition function for the antiferromagnetic state is greater than the other four states in this region.

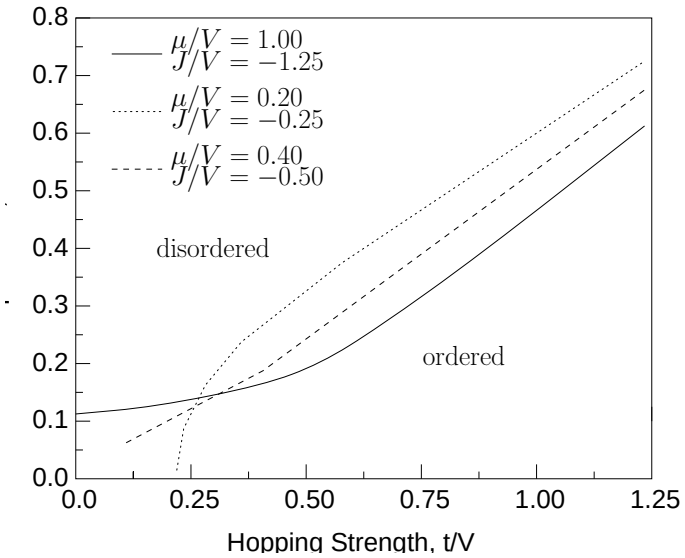

Figure 3.4: A cross section of the phase diagram of the 1D $t-J$ model for different values of μ/V and J/V.

In the intermediate region between the dotted line and the solid line, the value of t gets larger and J tends to go from negative values to the positive ones. However, the latter is rarely achieved, since the largeness of the other numbers prevents convergence. The fact that t gets large indicates that the holes enter the game, this time allowing the electrons to hop from one site to another. There are two possible candidates for the order in this region, one is shown in Figure 3.3(d), the other in Figure 3.3(e). The value of the partition functions for these two states tend to infinity after the first iteration. Hence, it is difficult to say which of the two the system will prefer. However, since J tends to go from negative values to positive ones, one may conclude that eventually the antiferromagnetic correlations become dominant, implying the order is of striped character shown in Figure 3.3(e).

Chapter 4

TWO-DIMENSIONAL *t-J* MODEL

This chapter presents the results of a research which is in progress. It is believed that the 2D $t-J$ model mainly captures the essential features of high temperature superconductivity. We report the results of a mean-field renormalization group theory of the 2D $t-J$ model, with the essential parts of the phase diagram. Just as in the 1D counterpart, one has a phase separation between an ordered phase and a disordered one, the ordered phase being of antiferromagnetic character in this case. This is in agreement with the results that the ground state of the 2D $t-J$ model is antiferromagnetic[23]. Because the computation time is large (approximately ten minutes for one iteration), a complete phase diagram is difficult to achieve. Hence, what happens between the ordered and disordered phases is still open.

4.1 Mean-Field Instead of Hard-Spin Mean-Field

Although hard-spin mean-field theory is more robust compared to mean-field theory, an application of it to the two dimensional $t-J$ model is not feasible because of computational limitations. To illustrate this fact, consider block spins made up of 3×3 blocks[1] at the boundary are interacting with hard-spins. Then, there is $0, \mp 1$. Since we have nine original spins, the hamiltonian describing the internal dynamics is a 3^9 by 3^9 matrix, a very large dimension indeed. In the numerical analysis we used, this matrix has to be generated for 3^9 times, a task which is impossible to implement. The block states used here are not 3×3 states, however a similar analysis shows that although not impossible, the computation time is still very large for our case. Therefore, when dealing with the interactions at the boundary, one is forced to use mean-field-like couplings to the outside, the essential feature is of Hartree-Fock type mentioned in the previous chapter. Our aim again is to achieve the block spin transformation by taking into account the effects at the boundaries, therefore being able to deal with the non-commutations at the two consecutive sites of the lattice.

4.2 Mean-Field Treatment of the Boundary

The $t-J$ model hamiltonian in 2D $t-J$ model is defined as:

$$H = -t\sum_{\langle ij\rangle,\sigma}(c^{\dagger}_{i\sigma}c_{j\sigma} + c^{\dagger}_{j\sigma}c_{i\sigma}) - J\sum_{\langle ij\rangle}\mathbf{S}_i\cdot\mathbf{S}_j + V\sum_{\langle ij\rangle}n_in_j + \mu\sum_i n_i, \qquad (4.1)$$

where the sums over $\langle ij\rangle$ is made over the nearest neighbor spins only. Just as in the one dimensional problem, double occupancies are not allowed. In the two dimensional version of the problem, we used the block states that are shown in Figure 4.1. In this figure, the capital letters (S's) stand for the real spins,

[1]The choice of blocks that are made up of three-site chains is compulsory in order that the states used in the renormalization group analysis preserve their forms under renormalization.

whereas the lowercase letters (m's) stand for the mean-field couplings to the outside. Also, the interactions between the real spins are shown by solid lines, and the couplings at the boundary to the mean-fields are shown by dashed lines. As will be shown later, this choice of the block spins preserves the ground states under renormalization, as well making the computational time lesser than of the other possibilities. With this choice, the hamiltonian matrix becomes a 243 by 243 matrix, since there are a total of $3^5 = 243$ different configuration of states.

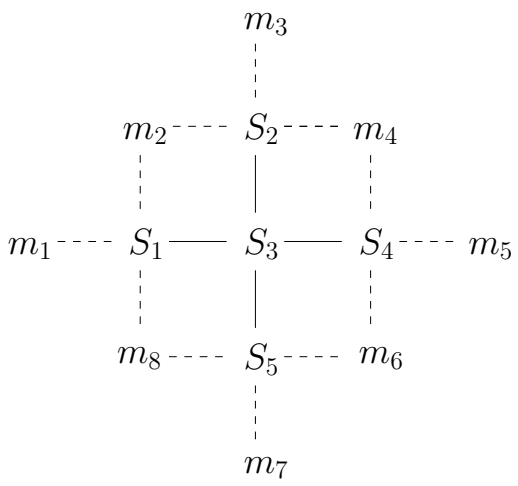

Figure 4.1: Block spin configuration that is used in the renormalization group theory of the 2D $t - J$ model.

The hamiltonian of the internal dynamics is calculated exactly as:

$$\begin{aligned} H_{\text{internal}} \quad = \quad & - \quad t(c^\dagger_{1+}c_{3+} + c_{1+}c^\dagger_{3+} + c^\dagger_{1-}c_{3-} + c_{1-}c^\dagger_{3-} \\ & + \quad c^\dagger_{2+}c_{3+} + c_{2+}c^\dagger_{3+} + c^\dagger_{2-}c_{3-} + c_{2-}c^\dagger_{3-} \\ & + \quad c^\dagger_{3+}c_{4+} + c_{3+}c^\dagger_{4+} + c^\dagger_{3-}c_{4-} + c_{3-}c^\dagger_{4-} \\ & + \quad c^\dagger_{3+}c_{5+} + c_{3+}c^\dagger_{5+} + c^\dagger_{3-}c_{5-} + c_{3-}c^\dagger_{5-}) \\ & - \quad J(\mathbf{S}_1 \cdot \mathbf{S}_3 + \mathbf{S}_2 \cdot \mathbf{S}_3 + \mathbf{S}_3 \cdot \mathbf{S}_4 + \mathbf{S}_3 \cdot \mathbf{S}_5) \\ & + \quad V(n_1n_3 + n_2n_3 + n_3n_4 + n_3n_5) \\ & + \quad \mu(n_1 + n_2 + n_3 + n_4 + n_5), \end{aligned} \tag{4.2}$$

where the meaning of each term has been explained in the previous chapter. Our next aim is to write a hamiltonian that takes into account the couplings to the outside. To do this, we first start by denoting the magnetizations at the

boundary by xm_i's, and mean occupations by xn_i's. The hopping term H_1 is treated separately, by considering whether the site to which an electron may hop is filled or not. The remaining part of the hamiltonian that couples to the outside can be written as:

$$\begin{aligned} H_2 &= -J\{(xm_1+xm_2+xm_8)S_{1z}+(xm_2+xm_3+xm_4)S_{2z} \\ &+ (xm_4+xm_5+xm_6)S_{4z}+(xm_6+xm_7+xm_8)S_{5z}\} \\ &+ V\{(xn_1+xn_2+xn_8)n_1+(xn_2+xn_3+xn_4)n_2 \\ &+ (xn_4+xn_5+xn_6)n_4+(xn_6+xn_7+xn_8)n_5\}. \end{aligned} \tag{4.3}$$

Then, the total hamiltonian becomes $H = H_{\text{internal}} + H_1 + H_2$. This hamiltonian is used for the calculation of the partition function $Z = \exp(-\beta H)$ in the forward renormalization. However, since the matrix is large in size, the exponentiation cannot be done with the direct Taylor series expansion because of computational limitations. For this purpose, another way has been implemented, which can be summarized as follows. First, the 243×243 matrix was reduced to a symmetric tridiagonal form by means of orthogonal similarity transformations. Second, the eigenvalues of this tridiagonal matrix is found by the so-called QL method, together with the eigenvectors of the hamiltonian matrix. Third, the exponential of the eigenvalues has been calculated. Finally, the exponential of the hamiltonian matrix was found by the operation:

$$\exp(H) = \sum_k \langle k|e^{\lambda_k}|k\rangle, \tag{4.4}$$

where $|k\rangle$'s are the eigenvectors and λ_k's are the eigenvalues of the hamiltonian.

4.3 Renormalization Group Procedure

4.3.1 Block Spin Rule and States

The majority rule for the two dimensional case is similar to the one dimensional case. When the number of any of the three different states is greater than or equal to 3, then the block spin that is formed by these states takes the value of these states as the block spin value. Another possibility is that any two of the three states may happen to be equal just as in the case of 2 pluses, 2 zeros and a single minus. In this case, the block spin value is the one that resides at the center of the block, no matter whether any of the two equally numbered states reside at the center or not. Since it is not possible to generate all the 243 different combinations of states here, we content with some examples to the block spin rule shown in Figure 4.2.

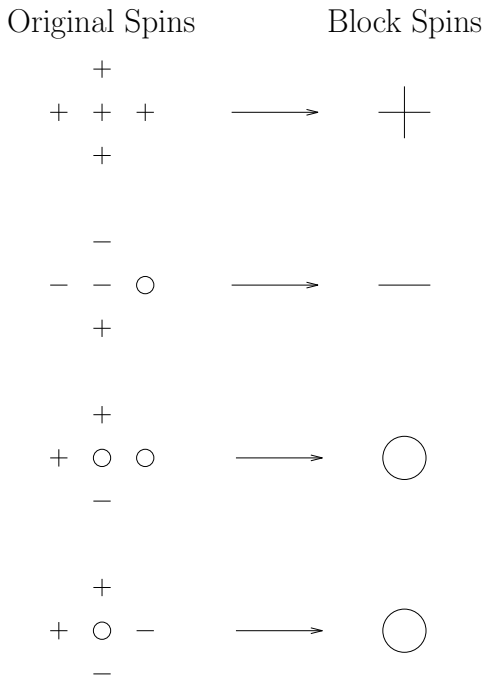

Figure 4.2: Examples to the majority rule for the 2D $t - J$ model.

The states used in the renormalization of the 2D $t - J$ model are analogs of the 1D case, again constructed in such a way as to preserve their form under repetitive renormalization group transformations. They are shown in Figure 4.3.

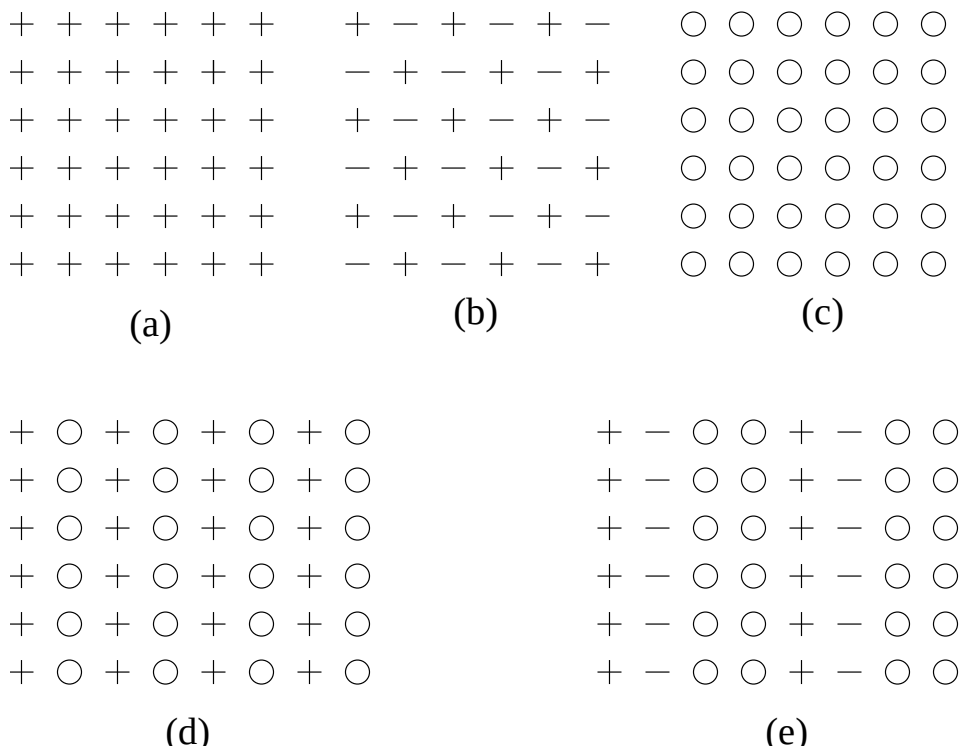

Figure 4.3: States that are used in the renormalization group procedure of the 2D $t-J$ model: (a) ferromagnetic state, (b) antiferromagnetic state, (c) empty state, (d) plus-hole state, (e) striped state.

4.3.2 Forward Renormalization

The forward renormalization is the same as that used in the one dimensional counterpart of the problem. We take the trace of the exponential hamiltonian over the block states. A typical renormalization is shown in Figure 4.4 for an arbitrary configuration of original spins in the lattice. The spins that are outside the block spins only contribute to the free energy and do not enter the renormalization. Another important difference from that of the 1D case is that this time the correction to the partition function due to the last term in the Hartree-Fock approximation comes from the mean-field interactions at the boundary. The unabridged form of this correction is very lengthy to give here, but for the S_1 site

shown in Figure 4.1, it becomes:

$$\begin{aligned} z_\mu &= \mathrm{Tr}_\mu \exp(-\beta H) \\ &\times \exp[t\sqrt{1-n_1}(\sqrt{xn_1}+\sqrt{xn_2}+\sqrt{xn_8})] \\ &\times \exp[t\sqrt{n_1}(\sqrt{1-xn_1}+\sqrt{1-xn_2}+\sqrt{1-xn_8})] \\ &\times \exp[\frac{1}{2}Jm_1(xm_1+xm_2+xm_8)] \\ &\times \exp[-Vn_1(xn_1+xn_2+xn_8)]. \end{aligned} \tag{4.5}$$

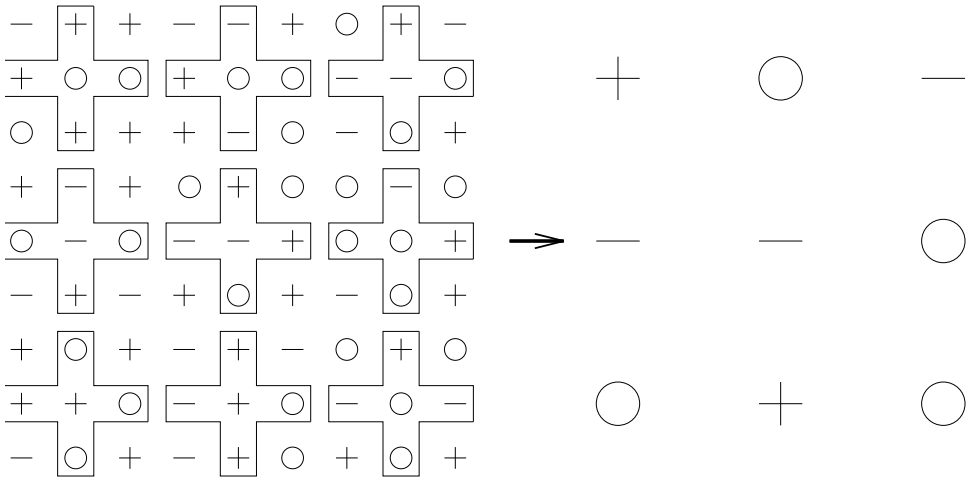

Figure 4.4: Forward renormalization of the 2D lattice.

4.3.3 Backward Renormalization

For the backward renormalization, we used a classical approximation in the calculation of free energies per site. In order to do this, one can take an arbitrary number of spins and evaluate the free energies using classical analog of the $t-J$ hamiltonian for the five different states that enter the renormalization. Then, the free energy per site, f, is given by:

$$f = \frac{\text{Free Energy}}{\text{number of spins}} \tag{4.6}$$

In our case, we chose a 4 by 4 lattice, a total of 16 spins. The free energies per site, as functions of the coupling constants, are calculated as follows:

$$Z_1' = \frac{3}{2}J + \frac{3}{2}V + \mu + g \tag{4.7}$$

$$Z_2' = -\frac{3}{2}J + \frac{3}{2}V + \mu + g \tag{4.8}$$

$$Z_3' = g \tag{4.9}$$

$$Z_4' = \frac{3}{4}t + \frac{3}{8}J + \frac{3}{8}V + \frac{1}{2}\mu + g \tag{4.10}$$

$$Z_5' = \frac{3}{8}t + \frac{3}{16}J + \frac{3}{16}V + \frac{1}{2}\mu + g \tag{4.11}$$

for the five states shown in Figure 4.3, respectively. The renormalization group equations have been found by equating the free energies of the renormalized and original systems. These equations are then solved numerically by the method Gaussian elimination method to give the renormalized coupling constants as functions of original ones. The fixed points and their physical meanings will be discussed in the following sections.

4.4 Fixed Points and Discussion

We have found three fixed points that are given in Table 4.1. The eigenvalues of the corresponding linearization matrices are given in Table 4.2. By looking at these eigenvalues, we see that the fixed point labeled by the "A" has complex conjugate eigenvalues with absolute values of the real parts less than one. Although this may be thought of as an indicative of a separatrix between ordered and disordered states, this cannot be the case because the fixed point itself resembles a high temperature fixed point. The fixed point "B" cannot be linearized in its neighborhood. It is possible that there is a singularity at that point, whose physics may be interesting. However, the computation time for just one iteration of the program is of the order of ten minutes, therefore making it almost impossible to examine what really goes on around this point. One more time note that the fixed point "C" has complex conjugate eigenvalues, hence there is a strong possibility that this points would correspond to a real separatrix between

a disordered and an ordered phase. Albeit the computation time is large, we were

	g	t	J	V	μ
A	-0.5490	0.0000	0.0000	0.0000	0.0000
B	0.0763	-1.865	2.2420	-0.6200	3.5820
C	0.0114	-0.9720	-0.4578	-0.2580	2.3550

Table 4.1: Fixed points that are found from the mean-field renormalization group theory of the 2D $t - J$ model.

able to check the high and low temperature behavior of the phase diagram. We note that there is indeed an antiferromagnetic phase for low temperatures as the t tends to zero and J diverges positively. Also, for points close to zero, it was seen that they eventually converge to the fixed point labeled with the letter "A". The intermediate physics may be interesting to observe, especially around the fixed points labeled with letters "B" and "C". In Figure 4.5, we give a qualitative picture of the phase diagram for the 2D $t - J$ model, with a question mark for the region that is still under investigation.

A	B	C
9.0000		8.9991
$0.8444 + 1.4958i$		-6.4371
$0.8444 - 1.4958i$		$2.1531 + 1.8450i$
-0.1467		$2.1531 - 1.8450i$
0.0016		$- 0.0811$

Table 4.2: Eigenvalues of the linearization matrices corresponding to the fixed points for the 2D $t - J$ model.

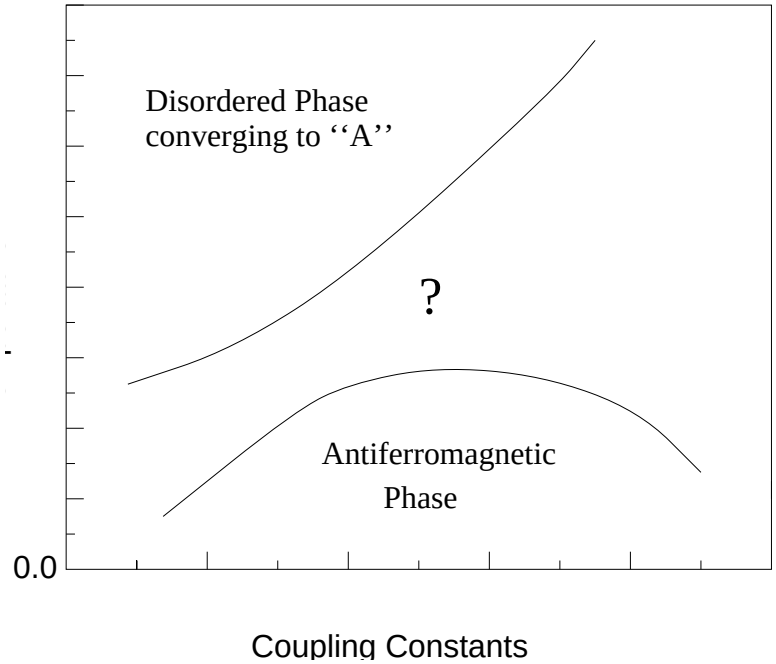

Figure 4.5: Qualitative picture of the phase diagram for the 2D $t-J$ model found by the mean-field renormalization group method.

Chapter 5

CONCLUSION

The quantum nature of the strongly correlated electronic systems makes it difficult to implement the various renormalization group techniques such as block spin transformation and Migdal-Kadanoff bond-moving technique. At this point, a novel study that combines the three important theories, namely, hard-spin mean-field theory, mean-field theory, and renormalization group theory is proposed and applied to the one and two dimensional $t - J$ models. The method presented here takes into account the noncommutations of the operators at the two consecutive sites of the square lattice on which these models are defined. This is achieved by replacing the real quantum interactions at the boundary by their Hartree-Fock approximated form, which is equivalent to replacing the commutators at the boundary by a c-number. One is then allowed to apply a block spin transformation over the lattice, resulting in renormalization group equations. The proposed method is a general one and can be applied to various low-dimensional model quantum systems.

Chapter 2 mainly deals with the high temperature superconductivity models, and gives detailed information about $t - J$ and Hubbard models. In this chapter, the hard-spin mean-field theory is discussed, with its overwhelming advantage over the conventional mean-field theory. A sample application of the former to the 2D Ising model is presented with results for the magnetization and free energy. In Chapter 3, the hard-spin mean-field theory is used as a tool to account

for the interactions at the boundary. This is done so by means of considering a three-site $t - J$ chain interacting at the boundaries with hard-spins. The robust nature of the hard-spin mean-field theory comes from the fact that it considers every possibility and disregarding none, by simply weighing the possibilities by a pre-defined probability function. The renormalization group transformation presented in this chapter is two-folded; while the "forward" renormalization calculates the free energies by taking the trace of the partition function over the block states, the "backward" renormalization calculates the same quantity for the original lattice by means of an approximation as discussed in the text. Then, by requiring that the two should be equal one arrives at the values of the renormalized coupling constants as functions of original ones. The investigation of the fixed points in the coupling constant space yields a finite temperature phase diagram for the one dimensional phase space. An ordered and a disordered phase is found, separated by different phase separation lines. The character of the ordered phase is investigated at different portions of the phase space, and it is found that it shows antiferromagnetic character in its ground state, as the value of t gets smaller and the value of J gets larger. This is verified by value of the free energy being less than that of the other possible candidates. In the intermediate region, it is mentioned that a striped phase may exist, as t tends to increase.

In Chapter 4, a similar method is applied to the two dimensional $t-J$ model. However, in dealing with the interactions at the boundary, mean-field theory is used instead of the more liable hard-spin mean-field field due to the limitations discussed in the text. Since the block spin used in the two dimensional problem consists of five real spins, the matrix in this case is a 243 by 243 matrix, whose exponential has to be generated numerous times in order to achieve convergence. An efficient method for this purpose is explained, which allows one to calculate the partition functions in an acceptable amount of time. The forward renormalization in the 2D case is exactly the same as that of the 1D case, while the backward renormalization makes use of a classical approximation in order to evaluate the value of the free energies per site. The renormalization group equations yield three fixed points in the two dimensional problem. The ground state is found to have an antiferromagnetic character, which is indeed thought to be the ground

state of the high-T_c cuprates. However, computation time limits the pace of the investigation, that is why we are content with presenting the qualitative features of the phase diagram only.

A next step may be the application of the method presented here to other models such as the Hubbard model which is thought to be more realistic than the $t - J$ model. Also, the quantum version of the hard-spin mean-field theory is a novel subject on its own, and may require further investigation by numerous applications to different quantum spin systems. This would clarify the advantages, or if exists, disadvantages of this theory in the quantum domain.

Appendix A

1D *t-J* MODEL

A.1 The Program

```
      common /hler/ h,eh
      common /debug/ ideb,istate,ispin,jspin
      dimension zz(5),istate(3,9),ispin(27),jspin(27)
      dimension h(27,27),eh(27,27)
      dimension xx(5),yy(5),e(5),b(5,5)
      dimension vf(5),vb(5),bf(5,5),bb(5,5)

      ideb=0

c  generate block states

      ...........

      open(1,file="tj.log",access="append")
      linear=0

    1 write(*,*)'enter g,t,j,v,mu: '
      read(*,*)g,t,xj,v,xmu

      write(*,*)' search for fp? (0 for no): '
      read(*,*)itest
      if(itest.ne.0)goto 3
      g=-5.

      write(1,*)'start: ',t,xj,v,xmu

      write(1,*)t,xj,v,xmu

    2 call rf(g,t,xj,v,xmu,zz)
      call rb(g,t,xj,v,xmu,zz)
```

```
      write(*,*)'t,j,v,mu: ',t,xj,v,xmu
      write(*,*)' one more loop? (0=no/1=yes/2=fixed point): '
      read(*,*)itest
      if(itest.eq.0)stop
      if(itest.eq.1)then
        g=-5.
        goto 2
      endif

c search for fp:
    3 xx(2)=t
      xx(3)=xj
      xx(4)=v
      xx(5)=xmu
      xx(1)=g

    4 write(*,*)'searching around ',xx
      write(1,*)'searching around ',xx

      t=xx(2)
      xj=xx(3)
      v=xx(4)
      xmu=xx(5)
      g=xx(1)

      call rf(g,t,xj,v,xmu,zz)
      call r(xx,yy)

      write(*,*)'old system: ',zz
      write(*,*)'new system: ',yy
      write(1,*)'old system: ',zz
      write(1,*)'new system: ',yy

      err=0.
      do i=1,5
        vf(i)=zz(i)
        vb(i)=yy(i)
        e(i)=zz(i)-yy(i)
        err=err+abs(e(i))
      enddo

      write(*,*)'error measure: ',err
   12 write(*,*)'continue? (0=stop/1=continue/2=linearize): '
      read(*,*)itest
      if(itest.eq.0)stop
      if(itest.eq.1)goto 11

      if(linear.eq.0)then
        write(*,*)'sorry, matrices not calculated or lost'
        goto 12
      endif
      linear=0
      call gelg(5,5,bb,bf,ier)
      if(ier.ne.0)then
        write(*,*)'inversion problem in gelg; ier=',ier
        goto 12
      endif
```

```
      do i=1,5
        write(*,800)(bf(i,j),j=1,5)
      enddo
      goto 12

  11  eps=0.001
      do i=1,5
        temp=xx(i)
        xx(i)=xx(i)+eps

        t=xx(2)
        xj=xx(3)
        v=xx(4)
        xmu=xx(5)
        g=xx(1)
        call rf(g,t,xj,v,xmu,zz)
        call r(xx,yy)

        do j=1,5
          b(j,i)=(zz(j)-yy(j)-e(j))/eps
          bf(j,i)=(zz(j)-vf(j))/eps
          bb(j,i)=(yy(j)-vb(j))/eps
        enddo
        linear=1

        xx(i)=temp
      enddo

c     do i=1,5
c       write(*,800)(b(i,j),j=1,5)
c     enddo
800   format(1p5e13.3)

      call gelg(5,1,b,e,ier)
      if(ier .ne. 0)then
        write(*,*)'ill defined b, ier=',ier
      endif

c     write(*,*)'correction: ',e

      err=0.
      do i=2,5
        if(err .lt. abs(e(i)) )err=abs(e(i))
      enddo

      if(err .gt. 0.1)then
        do i=1,5
          e(i)=0.1*e(i)/err
        enddo
c       write(*,*)'scaled to: ',e
      endif

      do i=1,5
        xx(i)=xx(i)-e(i)
      enddo

      goto 4
      end
```

A.2 Calculation of the Probability Function

The most general form of the probability function can be written as:

$$P(\sigma, m, n) = c_0 + c_1\sigma + c_2\sigma^2, \tag{A.1}$$

where c_0, c_1 and c_2 are constants. The values of these constants can be found by the method of Lagrange multipliers, subject to the conditions:

$$\sum_{\sigma=0,\mp1} P(\sigma, m, n) = 1, \tag{A.2}$$

$$\sum_{\sigma=0,\mp1} P(\sigma, m, n)\sigma = m, \quad \text{and} \tag{A.3}$$

$$\sum_{\sigma=0,\mp1} P(\sigma, m, n)\sigma^2 = n. \tag{A.4}$$

However, a more simple way is to proceed by inserting $P(\sigma, m, n)$ directly into these constraints. This gives:

$$3c_0 + 2c_2 = 1, \tag{A.5}$$

$$2c_1 = m, \tag{A.6}$$

$$2c_0 + 2c_2 = n. \tag{A.7}$$

These immediately yield $c_0 = 1 - n, c_1 = m/2, \text{and} c_2 = (3/2)n - 1$. Hence the probability function is found as:

$$P(\sigma, m, n) = (1 - n) + \frac{m}{2}\sigma + (\frac{3}{2}n - 1)\sigma^2. \tag{A.8}$$

Bibliography

[1] J.G. Bednorz and K.A. Muller, Possible High-T_c Superconductivity in the Ba-La-Cu-O System. *Zeitschrift für Physik B* **64**,189 (1986).

[2] H.K. Onnes, *Akad. van Wetenschappen (Amsterdam)* **14**,113 (1911).

[3] H. Takagi, S. Uchida, K. Kitazawa, and S. Tanaka, *Japanese Journal of Applied Physics* **26**, L123 (1987).

[4] L.N. Cooper, J. Bardeen, and J.R. Schrieffer, Theory of Superconductivity, *The Physical Review* **108**, 1175 (1957).

[5] J. Hubbard, Electron Correlations in Narrow Energy Bands, *Proceedings of the Royal Society* **A276**, 238 (1963).

[6] V.J. Emery, Theory of High-T_c Superconductivity in Oxides, *Physical Review Letters* **58**, 2794-2927 (1987).

[7] P.B. Littlewood, C.M. Varma, and E. Abrahams, Pairing Instabilities of the Extended Hubbard Model for Cu-O Based Superconductors, *Physical Review Letters* **63**, 2602-2605 (1989).

[8] V.J. Emery and G.Reiter, Mechanism for High-Temperature Superconductivity, *Physical Review B* **38**, 4547-4556 (1988).

[9] F.C. Zhang and T.M. Rice, Effective Hamiltonian for the Superconducting Cu-Oxides, *Physical Review B* **37**, 3759-3761 (1988).

[10] J.R. Schrieffer, X.-G. Wen, and S.-C. Zhang, Spin-Bag Mechanism of High-Temperature Superconductivity, *Physical Review Letters* **60**, 944-947 (1988).

[11] J.R. Schrieffer, X.-G. Wen, and S.-C. Zhang, Dynamic Spin Fluctuations and the Bag Mechanism of High-T_c Superconductivity, *Physical Review B* **39**, 11663-11679 (1989).

[12] A. Kampf and J.R. Schrieffer, Spectral Function and Photoemission Spectra in Antiferromagnetically Correlated Metals, *Physical Review B* **42**, 7967-7974 (1990).

[13] A.J. Millis, H. Monien, and D. Pines, Phenomenological Model of Nuclear Relaxation in the Normal State of $YBa_2Cu_3O_7$, *Physical Review B* **42**, 167-178 (1990).

[14] N.E. Bickers, D.J. Scalapino, and S.R. White, Conserving Approximations for Strongly Correlated Electron Systems: Bethe-Salpeter Equation and Dynamics for the Two-Dimensional Hubbard MOdel, *Physical Review Letters* **62**, 961-964 (1989).

[15] P. Monthoux, A. Balatsky, and D. Pines, Toward a Theory of High-Temperature Superconductivity in the Antiferromagnetically Correlated Cuprate Oxides, *Physical Review Letters* **67**, 3448-3451 (1991).

[16] P.W. Anderson, Two Crucial Experimental Tests of the Resonating Valance Bond-Luttinger Liquid Interlayer Tunneling Theory of High-T_c Superconductivity, *Physical Review B* **42**, 2624-2626 (1990).

[17] P.W. Anderson, "Luttinger-Liquid" Behavior of the Normal Metallic State of the 2D Hubbard Model, *Physical Review Letters* **64**, 1839-1841 (1990).

[18] R.B. Laughlin, *Science* **242**, 525 (1988).

[19] Y.-H. Chen, F. Wilczek, E. Witten and B.I. Halperin, *International Journal of Modern Physics B* **3**, 1001 (1989).

[20] X.-G. Wen, F. Wilczek and A. Zee, Chiral Spin States and Superconductivity, *Physical Review B* **39**, 11413-11423 (1989).

[21] N. Nagaosa and P.A. Lee, Normal State Properties of the Uniform Resonating-Valance-Bond State, *Physical Review Letters* **64**, 2450-2453 (1990).

[22] C.M. Varma, P.B. Littlewood, S. Schmitt-Rink, E. Abrahams and A. Ruckenstein, Phenomenology of the Normal State of Cu-O High-Temperature Superconductors, *Physical Review Letters* **63**, 1996-1999 (1989).

[23] E. Dagotto, Correlated Electrons in High-Temperature Superconductors, *Reviews of Modern Physics* **66**, 763-840 (1994).

[24] Gerald D. Mahan, Many-Particle Physics, 2nd Edition, *Plenum Press*, New York (1990).

[25] H.A. Bethe, *Z. Physik* **71**, 205-26 (1931).

[26] M. Ogata, M.U. Luchini, S. Sorella and F.F. Assaad, Phase Diagram of the One-Dimensional $t-J$ Model, *Physical Review Letters* **66**, 2388-2391 (1991).

[27] W.O. Putikka, M.U. Luchini and T.M. Rice, Aspects of the Phase Diagram of the Two-Dimensional $t-J$ Model, *Physical Review Letters* **68**, 538-541 (1992).

[28] V.J. Emery, S.A. Kivelson and H.Q. Lin, Phase Separation in the $t-J$ Model, *Physical Review Letters* **64**, 475-478 (1990).

[29] S.R. White and D.J. Scalapino, Density Matrix Renormalization Group Study of the Striped Phase in the 2D $t-J$ Model, *Physical Review Letters* **80**, 1272 (1998).

[30] S.Rommer, S.R. White and D.J. Scalapino, Phase Seperation in $t-J$ Ladders, *Physical Review B* **61**, 13424 (2000).

[31] C.S. Hellberg and E. Manousakis, Stripes and the $t-J$ Model, *Physical Review Letters* **83**, 132 (1999).

[32] G.B. Martins, C. Gazza, J.C. Xavier, A. Feiguin, and E. Dagotto, Doped Stripes in Models for the Cuprates Emerging from the One-Hole Properties of the Insulator, *Physical Review Letters* **84**, 5844 (2000).

[33] S. Sorella, G.B. Martins, F. Becca, C. Gazza, L. Capriotti, A. Parola, and E. Dagotto, Superconductivity in the Two-Dimensional $t-J$ Model, *cond-mat/0110460*, (2001).

[34] J.W. Halley, X-F Wang and S. Davis, Mean-Field Calculations of the Properties of the dilute $t - J$ Model for High-Temperature Superconductivity, *Physical Review B* **46**, 6560-6571 (1992).

[35] V.J. Emery and G. Reiter, Quasiparticles in the Copper-Oxygen Planes of High-T_c Superconductors: An Exact Solution for a Ferromagnetic Background, *Physical Review B* **38**, 11938-11941 (1988).

[36] F.C. Zhang and T.M. Rice, Validity of the $t - J$ Model, *Physical Review B* **41**, 7243-7246 (1990).

[37] V.J. Emery and G. Reiter, Reply to "Validity of the $t - J$ Model", *Physical Review B* **41**, 7247-7249 (1990).

[38] C. Gros, R. Joynt and T.M. Rice, Antiferromagnetic Correlations in Almost-Localized Fermi Liquids, *Physical Review B* **36**, 381-393 (1987).

[39] J. Cardy, Scaling and Renormalization in Statistical Physics, *Cambridge University Press*, Cambridge (1996).

[40] E. Ercolessi, G. Monardi, and P.Pieri, An Introduction to the Hubbard Model, in Strongly Correlated Magnetic and Superconducting Systems, G. Sierra, and M.A.M. Delgado, eds., *Springer-Verlag*, Berlin Heidelberg (1997).

[41] R.R. Netz and A.N. Berker, Hard-Spin Mean-Field Theory: Formulation for Ising, XY, and Other Models, *Journal of Applied Physics* **70** (10), 15 (1990).

[42] G. Migliorini, and A.N. Berker, Finite-Temperature Phase Diagram of the Hubbard Model, *unpublished*.

[43] A. Falicov, and A.N. Berker, Finite-Temperature Phase Diagram of the $t-J$ Model: Renormalization Group Theory, *Physical Review B* **51**, 12458-12463 (1995).